Aus dem Max-Planck-Institut für Psychiatrie

Geschäftsführende Direktorin: Prof. Dr. Dr. Elisabeth Binder

Do Long-Term Changes in Neuronal Activity Translate into Changes in Grey Matter Volume?

Dissertation

zum Erwerb des Doktorgrades der Medizin

an der Medizinischen Fakultät der

Ludwig-Maximilians-Universität München

vorgelegt von

Lea Marleen Joanna Bartmann

aus

Aschaffenburg

2025

Mit Genehmigung der Medizinischen Fakultät der

Ludwig-Maximilians-Universität zu München

Erster Gutachter:	PD Dr. Carsten Wotjak
Zweiter Gutachter:	Prof. Dr. Nikolaos Koutsouleris
Dritter Gutachter:	PD Dr. Robert Forbrig

Dekan:	Prof. Dr. med. Thomas Gudermann

Tag der mündlichen Prüfung: 23.10.2025

Abstract

The term “Schizophrenia” is commonly used to refer to a group of psychiatric disorders which share the same symptom pattern. Patients often suffer from thought disorders, hallucinations and psychoses and must deal with severe repercussions in their personal and professional lives. Schizophrenia affects around 1% of the world population and is associated with a reduced life expectancy of up to 13-15 years. According to literature, disturbances in the metabolism of nerves and imbalances of neurotransmitters are thought to be responsible for the development of schizophrenia, though the exact pathogenesis remains unknown.

Neuroimaging studies however identified a pattern of grey matter volume changes (GMV) in brains of schizophrenic patients, that correlates with the onset of schizophrenia. In the prodromal phase, hypermetabolism was detected in the hippocampal CA1 field, spreading to all hippocampal subregions throughout the course of disease. This hyperactivated state is accompanied by an initial increase in GMV, which later turns into volume reduction.

It is currently not known whether there is a causal relationship between increased neuronal activity and volume changes in the brain. The aim of my thesis was to investigate the consequences of increased, respectively decreased neuronal activity in the hippocampus on changes in GMV of efferent structures. Using a chemogenetic construct, longitudinal in-vivo magnetic resonance imaging (MRI) and voxel-based morphometry (VBM) analyses in mice, I was able to describe a trend in the relation between chronically altered neuronal activity and GMV changes: efferent brain structures in mice that were exposed to chronic hippocampal hyperexcitation, showed a loss in volume over time, whereas neuronal inactivation was associated with volume increase in nearly all efferent areas. These findings support the assumption that hippocampal overstimulation is mainly responsible for the occurrence of GMV changes as reported in schizophrenic patients.

Kurzzusammenfassung

Der Begriff „Schizophrenie“ beschreibt eine heterogene Gruppe an psychischen Erkrankungen, die sich unter anderem durch Denkstörungen, Halluzinationen, Psychosen sowie Affektverflachung und sozialem Rückzug auszeichnen. Sie betrifft circa 1% der Weltbevölkerung und geht aufgrund vieler Komorbiditäten mit einer verringerten Lebenserwartung von bis zu 13-15 Jahren einher. Bis heute ist die Ätiologie nicht vollständig verstanden, sodass von einer multifaktoriellen Genese ausgegangen wird und mehrere wissenschaftliche Hypothesen existieren.

Neuere Neuroimaging Studien beschrieben Volumenveränderungen im Hippocampus schizophrener Patienten, welche einem krankheitsspezifischen Mustern zu folgen scheinen. Im frühen Krankheitsstadium kommt es demnach zunächst in der CA1 Region und später im gesamten Hippocampus zu hypermetabolen Zuständen, welche anfängliche von einer Volumenzunahme begleitet sind. Im Laufe der Erkrankung zeigt sich jedoch ein signifikanter Volumenverlust. Hierbei gilt: je stärker der Volumenverlust ausgeprägt ist, desto stärker ist die Symptomatik. Ob ein kausaler Zusammenhang zwischen erhöhter neuronaler Aktivität und Volumenveränderungen im Gehirn vorliegt, ist aktuell jedoch nicht bekannt.

Ziel meiner Arbeit war es, die Folgen einer erhöhten bzw. verringerten neuronalen Aktivität im Hippocampus auf Veränderungen des GMV in efferenten Strukturen zu untersuchen. Mithilfe eines chemogenetischen Konstrukts, longitudinaler in-vivo-MRT und VBM-Analysen bei Mäusen konnte ich eine Beziehung zwischen chronisch veränderter neuronaler Aktivität und GMV-Veränderungen beschreiben: Efferente Gehirnstrukturen bei Mäusen, die chronischer hippocampaler Überstimulation ausgesetzt waren, zeigten im Verlauf einen Volumenverlust, während neuronale Inaktivierung mit einem Volumenzuwachs in nahezu allen efferenten Bereichen verbunden war. Dies unterstützt die Annahme, dass hippocampale Überstimulation hauptsächlich für das Auftreten von GMV-Veränderungen verantwortlich ist, wie sie bei schizophrenen Patienten beobachtet werden.

Content

Abbreviations

AA	anterior amygdaloid area
AAV	adeno-associated virus
AMPA	α-amino-3-hydroxy-5-methyl-4-isoxazolepropionic acid
BMA	basomedial amygdaloid nucleus
BNST	bed nucleus of the stria terminalis
CA	cornu ammonis
CaMKII	Ca^{2+}/calmodulin-dependent protein kinase II
CLZ	clozapine
CNO	clozapine-N-oxide
CP	caudoputamen
Cr	creatine
DA	dopamine
DAPI	diamidino-2-phenylindole
DG	dentate gyrus
DREADD	designer receptors exclusively activated by designer drugs
ENT	entorhinal cortex
EPM	elevated plus maze
EPS	extrapyramidal symptoms
EPSP	excitatory postsynaptic potential
GABA	gamma-aminobutyric acid
Glu	glutamate
GMV	grey matter volume
GPCR	G protein-coupled receptors
hM3Dq	AAV8-CamKII-hM3Dq-mCherry (excitatory DREADD)
hM4Di	AAV8-CamKII-hM4Di-mCherry (inhibitory DREADD)

HPC	hippocampus
LS	lateral septum
LOT	lateral olfactory trac
LTD	long-term depression
LTP	long-term potentiation
Me	medial amygdaloid nucleus
MOB	main olfactory bulb
mPFC	medial prefrontal cortex
MRI	magnet resonance imaging
MRS	magnet resonance spectroscopy
MS	medial septum
NAAG	N-acetylaspartylglutamic acid
NAc	nucleus accumbens
NMDA-R	N-methyl-D-aspartate receptor
NRHypo	NMDA receptor hypofunctioning
OFT	open field test
PV+	parvalbumin positive
RDoC	research domain criteria initiative
SEM	standard error of the mean
SIT	social interaction task
SNr	substantia nigra
Sub	subiculum
Tau	taurine
TS	triangular septal nucleus
VBM	voxel-based morphometry
vP	ventral pallidum
VTA	ventral tegmental area

1. Introduction

1.1 Origin and Evolution of the Term “Schizophrenia”

In the German-speaking world, the understanding of psychiatric illnesses in the 19th century was mainly shaped by the principle of *unitary psychosis*. Accordingly, all different variants of psychiatric symptoms were seen as manifestations of one single psychiatric disorder. It was not until the late 1860s, that clinical studies suggested the existence of more than one psychiatric disorder, leading to the dismissal of the principle (Hecker 1871; Kahlbaum 1874). During this time, the psychiatrist Emil Kraepelin (1856 –1926) was convinced that somatic causes underlie all psychiatric disorders. To prove his theory, he conducted independent clinical longitudinal studies from 1883 on, resulting in classification systems for mental illnesses. Since then he constantly revised and refined his nosology (Kraepelin 1909-1915). In a modified form, the concept of Kraepelin´s nosology is still incorporated into today's clinical classification guidelines (ICD-10).

Innovative about Kraepelin’s nosology was, that it firmly linked diagnosis to prognosis. According to his dichotomy, endogenous psychoses can be divided into two distinct psychotic disorders: *“manic-depressive psychosis”* and *“dementia praecox”.* He believed that both were caused by yet undetectable physical and biological changes and distinguishable based on their prognosis. The manic-depressive psychosis, today known as “affective disease”, was said to be phasic with a good prognosis of recovery and no preferred age of onset. Dementia praecox, on the contrary, was characterised by a progressive course, early onset, and a poor prognosis. Dementia praecox is nowadays known as the first description of schizophrenia. Eugen Bleuler (1857-1939) disagreed with the concept of dementia praecox and the ability to invariably derive a firm prognosis from it. In 1911, he introduced the term "schizophrenia" for the first time to emphasise that schizophrenia is a heterogeneous group of illnesses (Bleuler 1911).

1.2 Classification of Symptoms

In the diagnostics of schizophrenia, Bleuler differentiated between specific *basic symptoms*, which are always present in a progressed state and unspecific *accessory symptoms*. This classification was refined by another psychiatrist named Kurt Schneider (1887-1967). Schneider distinguished between first and second-rank symptoms (Schneider 1950). Parts of first-ranked symptoms like auditorial hallucinations, thought withdrawals, insertion and interruption, thought broadcasting and delusional perception are still listed in the group (a) to (d) of specific symptoms in the latest ICD-10 code (see Table 1).

Today, schizophrenic experiences are also categorized as positive symptoms (delusions, hallucinations, thought disorder), negative symptoms (loss of motivation, apathy, social withdrawal) or cognitive dysfunction (lack of attention, memory, cognitive flexibility) (Gaebel 2010).

Table 1: ICD-10 Criteria of Schizophrenia (F20.x) (WHO et al. 1992)

Although no strictly pathognomonic symptoms can be identified, for practical purposes it is useful to divide symptoms into groups that have special importance for the diagnosis and often occur together, such as:
a) thought echo, thought insertion or withdrawal, and thought broadcasting;
b) delusions of control, influence, or passivity, clearly referred to body or limb movements or specific thoughts, actions, or sensations; delusional perception;
c) hallucinatory voices giving a running commentary on the patient's behaviour, or discussing the patient among themselves, or other types of hallucinatory voices coming from some part of the body;
d) persistent delusions of other kinds that are culturally inappropriate and completely impossible, such as religious or political identity, or superhuman powers and abilities (e.g. being able to control the weather, or being in communication with aliens from another world);
e) persistent hallucinations in any modality, when accompanied either by fleeting or half-formed delusions without clear affective content, or by persistent over-valued ideas, or when occurring every day for weeks or months on end;
f) breaks or interpolations in the train of thought, resulting in incoherence or irrelevant speech, or neologisms;
g) catatonic behaviour, such as excitement, posturing, or waxy flexibility, negativism, mutism, and stupor;

h) "negative" symptoms such as marked apathy, paucity of speech, and blunting or incongruity of emotional responses, usually resulting in social withdrawal and lowering of social performance; it must be clear that these are not due to depression or to neuroleptic medication;

i) a significant and consistent change in the overall quality of some aspects of personal behaviour, manifest as loss of interest, aimlessness, idleness, a self-absorbed attitude, and social withdrawal.

The normal requirement for a diagnosis of schizophrenia is that a **minimum of one** very clear symptom (and usually two or more if less clear-cut) belonging to any one of the groups listed as **(a)** to **(d)** above, or symptoms from at **least two** of the groups referred to as **(e)** to **(h),** should have been clearly present for most of the time during a period of **1 month** or more.

1.3 Burden of Schizophrenia

Schizophrenia affects around 1 % of the world population, regardless of country, culture or climate zone. Depending on the severity of schizophrenic symptoms, patients' lives are significantly affected. According to the long-term study conducted by Gerd Huber, only 56 % of schizophrenic patients achieve “social recovery”, meaning full employment at previous levels or below (Huber, Gross, and Schüttler 1979). Hence 44 % have limited employment or completely lose their ability to work. Schizophrenia also has one of the highest mortality rates of all psychiatric diseases as it is associated with social descent and a variety of comorbidities. Schizophrenic patients are for instance at increased risk for alcohol and substance abuse, anxiety, eating disorders as well as diabetes and cardiovascular disorders (Lu et al. 2022). Cancers are also more common due to poorer lifestyle and reduced health-seeking behaviours. The risk of suicide is increased by as much as 22 times compared to the general population, all of which add up to 13 - 15 years of potential life loss (Hjorthøj, Stürup, McGrath, and Nordentoft 2017).

Furthermore, schizophrenia tends to first appear in young adults with men being affected earlier (late adolescence to early twenties) than women (early twenties to early thirties) (Gaebel 2010). It typically emerges from an early prodromal phase with symptoms not or only partially present to a symptomatic and eventually chronic stage. Treatment response is hereby significantly affected by the duration of active illness prior to treatment (Lieberman et al. 2018). Severity and persistence of the symptoms thus determine the prognosis. Patients diagnosed and treated at an early-stage benefit greatly as they are more likely to experience remission and recovery (Lieberman et al. 2018; McHugo et al. 2018; NIH 2020). But the initial diagnosis is still based on the observation of symptoms and patient´s report. As a result, the point in time of diagnosis is often delayed to a stage of already progressed biological changes, where treatment becomes more challenging. Yet no specific diagnostic tests based on molecular or bioimaging procedures are available. This is mainly due to the non-specificity and heterogeneity of symptoms and the lack of knowledge about the pathophysiological mechanism. But without a profound knowledge of the causes of the disease, no specific drug therapy nor

specific diagnostic tools can be developed. Further research to identify the causes and potential targets is therefore urgently needed. However, the exploration and modulation of brain abnormalities or potential therapeutic targets usually requires animal models. This poses a major challenge given that schizophrenia is a uniquely human disorder.

1.4 Therapy of Schizophrenia

According to the fist-line therapy, treatment of schizophrenia consists primarily of medication with antipsychotics, also known as neuroleptics or major tranquillizers. They are used in the acute treatment and relapse prevention. Psychotherapeutic measures such as psychoeducation or cognitive behavioural therapy are used in addition to medication as a supportive measure and are important elements in long-term therapy.

To date, antipsychotic drugs can only supress but not eliminate symptoms due to poor understanding of the pathophysiology of schizophrenia. The aim of treatment is therefore to reduce suffering and improve functioning in social and cognitive spheres. Pharmacologically, most of the antipsychotics alter the effects of dopaminergic neurotransmission in the brain by targeting dopamine receptors. The blockade of dopamine D2 receptors in the mesolimbic pathway is hereby believed to be responsible for the strong antipsychotic effect and thus for the reduction of positive symptoms (Stępnicki, Kondej, and Kaczor 2018). Currently there are three generations of antipsychotics at disposal:

1) First generation antipsychotics (1960´s), like chlorpromazine or haloperidol, act as dopamine D2 receptor antagonists. Unfortunately, they do not interfere in the mesolimbic pathway only but affect dopamine receptors in other regions of the central nervous system too. For this reason, they can cause severe neurological side effects by blocking D2 receptors in the nigrostriatal pathway causing Parkinson-like extrapyramidal symptoms (EPS) or in the tuberoinfundibular pathway causing increased prolactin levels (Stępnicki, Kondej, and Kaczor 2018). Today, they have mainly been replaced by second-generation antipsychotics as treatment of choice.

2) Second-generation antipsychotics (1990´s) like clozapine, olanzapine or risperidone are characterised by an improved ratio between antipsychotic efficacy and risk of side effects. They operate as multi-target antagonists and show greater affinity to serotonin 5-HT_{2A} receptors than to dopamine D2 receptors.
3) The next, or third generation of antipsychotics (today), e.g. aripiprazole is characterised by its partial D2 agonist effects.

Although next-generation antipsychotics were developed to address the shortcomings of first-generation antipsychotics, they also have significant limitations. Patients continue to face side effects, including metabolic syndromes, cognitive impairments, sedation, weight gain, and sexual dysfunction. The need for many patients to undergo lifelong treatment for relapse prevention, exacerbates the imbalance between side effects and treatment benefits. This often leads to a loss of compliance. Additionally, while antipsychotics are frequently efficient in reducing severe positive symptoms, they lack the ability to control negative and cognitive ones (Mailman and Murthy 2010; Stępnicki, Kondej, and Kaczor 2018). One of the biggest challenges however remains the high percentage of up to 30 % of treatment-resistant patients (Kätzel, Wolff, Bygrave, and Bannerman 2020). Unfortunately, there currently exists no alternative to these broad-acting antipsychotic drugs. Therefore, new and more specific therapeutic approaches with fewer side effects and higher efficacy are needed, requiring a deeper understanding of the pathophysiology of schizophrenia.

1.5 Aetiology of Schizophrenia

In accordance with Bleuler's conception of schizophrenia as a heterogeneous group of diseases, it is assumed that schizophrenia has a multifactorial genesis with different pathogenetic factors being present in different subtypes. The “vulnerability-stress model” is often used to better understand schizophrenia and its interplay between nature and nurture and the underlying mechanism (Zubin and Spring 1977). Accordingly, neuropathological and / or biochemical changes in the brain occur due to genetic and developmental biological factors. Schizophrenia is considered a

highly heritable disease. A genome-wide association study identified 108 schizophrenia-associated genetic loci of which 75 % include protein-coding genes (Ripke et al. 2014). Notably, many of those are involved in glutamatergic neurotransmission, synaptic plasticity or encode voltage-gated calcium channel subunits. Genetic factors are seen as diathesis or predispositions, which can be triggered by external factors.

Examples of environmental risk factors for schizophrenia are childhood trauma and social adversities, obstetric complications, infections during pregnancy, migration, cannabis-intake or social isolation (Stilo and Murray 2019). In patients exposed to environmental risk factors, the prodromal onset of schizophrenia occurs about 8 years earlier than in patients with no environmental risk factors (Stepniak et al. 2014). Noteworthy, even pre- and perinatal events can increase the risk of developing schizophrenia (Sørensen et al. 2010).

These findings led to the neurodevelopmental approach, which assumes that disturbances at critical early stages of brain development cause schizophrenia. Schizophrenia may rather be seen as a developmental disorder than a classic degenerative disorder, as typical neurodegenerative characteristics such as gliosis, the proliferation of glia cells, are absent. It is also increasingly associated with the group of synapthopathies, which involve shrinkage of the neuropil, meaning synapses, axons, dendrites as well as glia cells (Harrison 2004).

Cytoarchitectural abnormalities and neuroradiological findings further link the brain developmental hypothesis to network dysfunction. There are developmental abnormalities, for example misplaced and aberrantly clustered neurons, that can be found in the hippocampal formation of schizophrenic patients (S.E. Arnold, Hyman, Van Hoesen, and Damasio 1991; Falkai, Schneider-Axmann, and Honer 2000). Cytoarchitectural abnormalities in the hippocampal formation (see Figure 1) can contribute to network dysfunction and abnormal function. The hippocampus in general is a brain region of particular interest in the pathophysiology of schizophrenia.

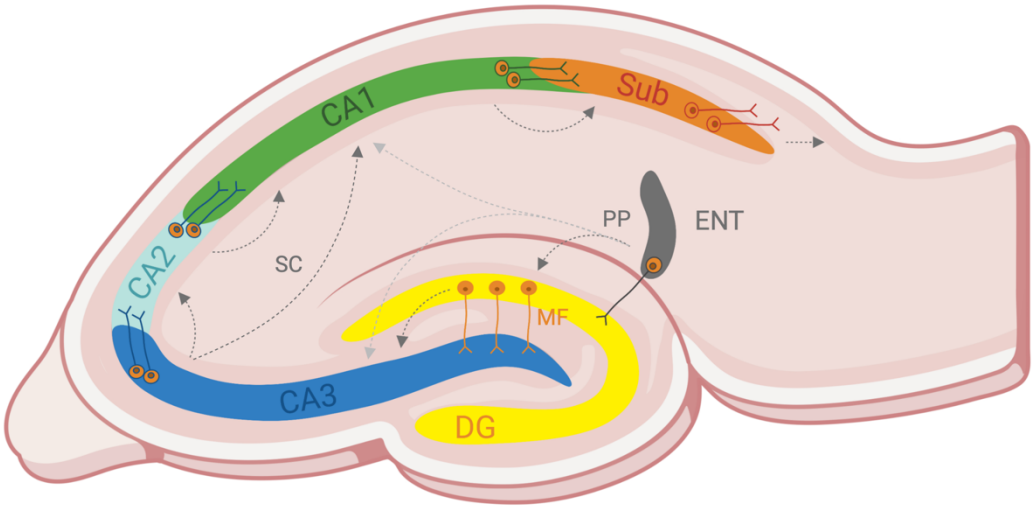

Figure 1: The Hippocampal Formation in a Mouse Brain is located in the medial temporal lobe and arranged along a dorsal-to-ventral axis (homologous to the posterior-to-anterior longitudinal axis in humans). The hippocampal structure of rodents corresponds to that of humans. It is composed of functional distinct subregions that receive subcortical and cortical inputs via the entorhinal cortex (ENT). Information, with respect to the anatomical gradient, is then transmitted via the perforant pathway (PP) to the dentate gyrus (DG). This marks the start of the so-called “trisynaptic pathway”. The DG then sends projections via the mossy fibre (MF) to the CA2 and CA3, CA3 via the Schaffer collateral (SC) to the CA1 and CA1 lastly to the subiculum (Sub). The CA1 and Sub hereby represent the main hippocampal output regions with efferences to many cortical and subcortical domains and returning ones to the ENT (adapted from (Neves, Cooke, and Bliss 2008). (Illustration created using BioRender.com)

1.5.1 Dopaminergic Hypothesis of Schizophrenia

Antipsychotics can decrease dopamine signalling by interfering with D2 receptors, resulting in the reduction of positive schizophrenic symptoms (see Chapter 1.4). A hyperdopaminergic state has therefore been linked to the onset of psychotic symptoms, leading to the initial description of the dopaminergic hypothesis. Another supporting fact is that amphetamine, which enhances dopamine release, may induce psychosis. Interestingly, amphetamine increases dopamine release in patients with schizophrenia significantly greater than in healthy patients (Grace 2012). However, antipsychotic effect occurs only after days or weeks while the drugs exert their pharmacological effect within hours. In addition, dopamine receptor antagonists

are not clinically effective at treating all aspects of schizophrenia. They do not act on negative and cognitive symptoms (Bygrave et al. 2019; Stępnicki, Kondej, and Kaczor 2018). These findings therefore suggest an abnormal modulation or increased responsivity of the dopamine system.

Hence, the cause of the disease cannot exclusively be explained by a primary dysfunction of the dopaminergic system. A network dysfunction involving multiple neurotransmitter systems, in particular the glutamatergic one, is nowadays considered to be more likely.

1.5.2 Glutamatergic Hypothesis of Schizophrenia

Glutamate (Glu) is ranked among the main excitatory neurotransmitters and is crucial for normal brain and body functions. It is essential in the regulation of pathways that connect, for example, the cortex, the limbic system, and thalamus regions. On the post-synapse, glutamate is detected among others by inotropic transmembrane receptors, the NMDA receptors (N-methyl-D-aspartate) and the AMPA receptors (α-amino-3-hydroxy-5-methyl-4-isoxazolepropionic acid). The association of glutamate dysfunction with schizophrenia mainly derives from clinical effects of NMDA receptor antagonists such as phencyclidine (PCP) and ketamine. Unlike the dopaminergic agonist amphetamine, which can only replicate positive symptoms, PCP or ketamine mimic a more comprehensive picture of schizophrenia (Javitt and Zukin 1991). They induce positive and negative symptoms as well as typical neurophysiological deficits by causing an increase in extracellular glutamate levels (Schobel et al. 2013).

The precisely coordinated interplay between inhibitory interneurons and excitatory pyramidal cells in the hippocampus is essential for normal brain functioning. A human hippocampus consists of approximately 10 million neurons. Large, glutamatergic pyramidal neurons account for around 90 %, the remaining 10 % are small, gamma-amino-butyric acid (GABA)ergic interneurons. Notably, NMDA channels strongly contribute to the excitatory postsynaptic potential (EPSP) in inhibitory interneurons (see Figure 2) and are crucial for their activation (Olbrich and Braak 1985). They are defined as fast-spiking and contain parvalbumin (PV+), a protein that binds Ca^{2+}. Fast-spiking interneurons are responsible for

the regulation of overall pyramidal firing (Lisman et al. 2008), as they are synaptic connected with glutamatergic pyramidal cells (see Figure 2). They act as sensors that monitor the activity of pyramidal cells. Under physiological conditions, interneurons use their NMDA receptors to sense present glutamate levels which are generated by active pyramidal cells. When glutamate levels reach a certain threshold, NMDA receptors will enhance the activation of interneurons. This leads to an increased GABAergic inhibition of pyramidal cells. The mechanism therefore ensures homeostasis and prevents excitotoxicity.

According to the NMDA receptor hypofunction theory (Lisman et al. 2008), malfunctioning of the NMDA receptors in the PV+ interneurons of the hippocampal CA1-subfield is considered to be causing schizophrenia.

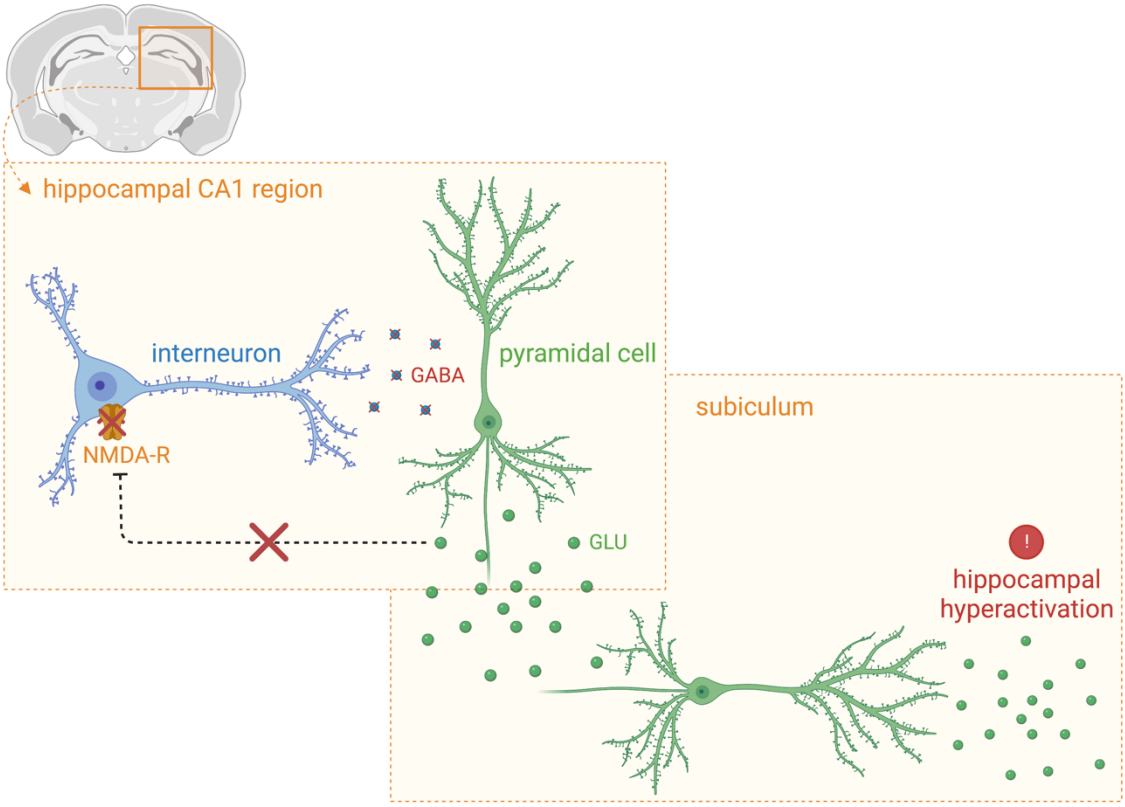

Figure 2: Illustration of the NMDA Receptor Hypofunction Theory Interneurons lose their ability to measure and modulate the glutamate levels (GLU), because the NMDA receptors (NMDA-R) are malfunctioning. As a result, interneurons will not inhibit the pyramidal cells in the CA1 region, leading to an inadequate overactivation of pyramidal cells in the subiculum and thus to hippocampal hyperactivation. (Illustration created using BioRender.com)

Malfunctioning leads to interneurons losing their ability to detect the actual level of glutamate. They erroneously assume a lack of pyramidal cell activity and consequently reduce their inhibitory output. This maladaptive disinhibition then causes an excitation-inhibition imbalance. As a result, pyramidal cells are overactive, which leads to an abnormal hippocampal firing pattern with excessive dysrhythmic excitatory output (Bygrave et al. 2019; Grace 2017; R.S. Kahn and Sommer 2015; Lisman et al. 2008). The hippocampal CA1 region possesses the largest number of interneurons among all hippocampal subfields with a great density of NMDA receptors. It is therefore especially vulnerable to receptor malfunctioning.

Support for the theory of NMDA hypofunctioning also comes from genetic evidence and post-mortem findings. In schizophrenic patients, reduced concentration of GABA in cortical regions and reduced activity and concentration of the synthesizing enzyme glutamate decarboxylase (GAD) and PV are reported (Lisman et al. 2008). Notably, GAD67 and PV are mainly located in hippocampal CA2/3, CA1 and cortical regions. Reduced expression of obligatory NMDA receptor subunits such as GluN1, GluN2C and GluN2A located on PV+ interneurons and abnormal activity of GABAergic interneurons in general were also observed (Bygrave et al. 2019). These deficits are not equally detectable in all cortical interneurons, but site-specific in hippocampal fast-spiking interneurons (Lisman et al. 2008). Interestingly, post-mortem studies reveal significantly reduced numbers of PV+ interneurons in hippocampi of schizophrenic patients (Grace 2017; Konradi et al. 2011; Lieberman et al. 2018).

Fast spiking interneurons are of extreme importance for the homeostatic regulation of pyramidal cells via negative feedback. Thus, they are significantly involved in controlling the brain's firing and network activity. Other processes, such as gamma oscillations, a synchronic firing pattern of pyramidal cells which is vital for temporal encoding and recalling of information, depend greatly on interneurons (Bygrave et al. 2019; Ho et al. 2017; Lisman et al. 2008; Nguyen et al. 2014). Therefore, the cooccurrence of dysfunctional, hypoactivated interneurons and reduced brain volume within the same area, strongly indicates a key role of the hippocampal neuronal activity in the

pathogenesis of schizophrenia (Ho et al. 2017; Konradi et al. 2011; McHugo et al. 2018; Small et al. 2011).

1.5.3 Volumetric and Metabolic Changes in the Hippocampus

The hippocampal formation modulates various brain processes in different regions via its widely ramified synaptic network. While the anterior hippocampus (= ventral in mice) is involved in stress, emotion, and anxiety-related behaviour, the posterior parts (= dorsal in mice) are associated with spatial navigation, storing and recalling of episodic memory and cognitive processing (Nakahara, Matsumoto, and van Erp 2018; Neves, Cooke, and Bliss 2008; Small et al. 2011; Haukvik et al. 2015). The hippocampus also influences novelty detection processes and salience attribution using its polysynaptic pathways to the ventral tegmental area (VTA).

In research, MRI is used to identify structural brain changes in a non-invasive manner. The differences in the volume of brain regions between experimental groups can be detected using VBM, which statistically compares high-resolution structural images (Keifer et al. 2015). A voxel hereby represents the smallest unit of a three-dimensional image. Region-specific changes in brain metabolism can be detected using magnetic resonance spectroscopy (MRS).

In the early stages of schizophrenia, elevated blood flow, metabolism, and glutamate levels are measured in the anterior hippocampal CA1 subregion. (Lieberman et al. 2018; Schobel et al. 2013). As the disease progresses, hypermetabolism spreads to other parts of the hippocampus such as the subiculum. Schizophrenic patients not only show hippocampal hyperactivity, correlating with psychosis (Heckers 2001; Grace 2012), but hippocampal volume reduction after psychosis onset (Nelson, Saykin, Flashman, and Riordan 1998; Heckers 2001; Lieberman et al. 2018; Schobel et al. 2013). Thus, hypermetabolism at basal state entails hippocampal volume reduction and precedes atrophy. With time, the focal atrophy expands across all hippocampal subfields, irrespective of medical treatment. The anatomical overlap of both, hippocampal hypermetabolism and volume reduction therefore suggests a common pathophysiologic mechanism. Furthermore, hippocampal involvement is neither a consequence of the disease

nor of treatment, as reduced hippocampal volume can already be observed in untreated patients in the prodromal stage and first episode (Harrison 2004; Bogerts et al. 1990; Pantelis et al. 2003).

In chronic schizophrenia, a negative correlation between duration, volume reduction and worsening of symptoms has been observed (Ho et al. 2017). More specifically, bilateral CA2/3, CA1 and bilateral subiculum volumes were negatively correlated with positive symptom severity (Kühn et al. 2012; Mathew et al. 2014).

These findings support the hypothesis that increased glutamate levels and the following repeated hyper-glutamatergic events provoke hippocampal hypermetabolism and atrophy in the CA1 and subiculum. The underlying mechanism of hippocampal GMV changes in the hippocampus of schizophrenic patients, however, remains unclear and the question of whether chronically increased neuronal activity is primarily responsible, unanswered.

1.6 Animal Models of Schizophrenia

Classification systems such as the ICD-10 or the “Diagnostic and Statistical Manual of Mental Disorders” (DSM-5) for psychiatric disorders still rely on the expression and variation of self-reported or observed symptoms. They facilitate diagnostic processes, treatment plans as well as the unification and statistical comparisons of data. Up to this day however, the understanding and treatment of mental disorders significantly fall behind that of other medical conditions. This is primarily because ICD diagnoses don’t correspond to distinct pathophysiological mechanisms. The fundamental issue of these wide-ranging diagnostic criteria becomes particularly evident in the research of schizophrenia.

Schizophrenia is one of the most heterogenous and complex mental disorders. Patients may share the same diagnosis, although they have only few symptoms in common. They can simultaneously meet the criteria for more than one mental disorder. The heterogeneity of disorders and the comorbidity across diagnoses, pose a major challenge for psychiatric research as creating a suitable animal model is extraordinary difficult. In general, animal models provide unparallel insight into pathophysiological mechanisms and are an

essential part of basic research. They not only allow for more rapid monitoring and controlled interference in neurobiological processes but permit invasive studies of structural and molecular changes. They also allow relatively easy real-time monitoring across the development of the disease and molecular analyses of the tissue. Three validity criteria are usually used to evaluate the utility and translational value of animal models. The criteria of *face validity* assess the correspondence of the model to the clinical presentation. The criteria of *construct validity* evaluates the replication of neurochemical and structural features of the disease and the criteria of *predictive validity* the predictability of its pharmacological response (Willner 1986). Mental illnesses like schizophrenia, however, are uniquely human disorder as they include symptoms like auditory hallucinations and paranoid delusions. Developing an animal model for schizophrenia that meets all three criteria is therefore rarely achievable. Hence, staying within the imprecise boundaries of existing disease classifications tremendously impedes the informative value of psychiatric studies (Anderzhanova, Kirmeier, and Wotjak 2017).

The National Institute of Mental Health (NIMH) therefore developed the “Research Domain Criteria Initiative” (RDoC), a more dynamic, dimensional, and open-minded research framework (National Institute of Mental Health 2022). RDoC shifts the focus from DSM-defined diseases to behavioural and neurobiological phenotypes, promoting studies in non-human models to investigate disease-specific hypotheses, underlying biological mechanisms, and behaviours. Researchers are hereby encouraged to use all available opportunities and modern research methods (Simmons and Quinn 2014). The framework includes *domains* of human functioning such as systems of emotion, motivation, or social behaviour. The mechanisms and behavioural elements within each domain are called *constructs*. They are measured along a span from normal to abnormal in environmental and neurodevelopmental context. The methods of measuring the mechanism are termed *units of analysis*, which include neurocircuit and behavioural assessments. The framework is dynamic and evolves according to new findings and emerging research (National Institute of Mental Health 2022).

In this study, I used MRI analyses to investigate long-term changes in neuronal activity as one potential mechanism underlying schizophrenia. As a model organism, I used C57BL/6N mice and equipped them with chemogenetic constructs that allowed the simulation of hippocampal hyper- and hypoactivation. The circuit of interest was therefore said to be the hippocampus, with pyramidal cells being targeted. MRI and MRS served as units of analysis. A control group was integrated, and behavioural tests performed to check for possible side effects of the chemogenetic constructs.

1.7 Aims of the Study

Specific patterns of morphological brain changes are found in many patients suffering from schizophrenia. So far, different mechanisms are being discussed as the driving force, none of which has yet been identified as a definite cause. This study aimed to investigate the question of whether long-term changes in hippocampal neuronal activity are linked to biphasic GMV-changes in schizophrenic patients. It focused on the following hypotheses:

1. In mice with hyperactivated hippocampal pyramidal neurons (hM3D group), I expected to detect an increase in excitatory transmission (elevated glutamate levels) and an increase in GMV in efferent brain structures during MRI2 (early phase). As time progresses, ongoing hyperexcitation was expected to trigger homeostatic plasticity as neurons are forced to protect themselves against excitotoxicity. Adaptive changes, for instance, include reduced synaptic contacts or shrunken dendritic spines, consequently resulting in a reduction of GMV in MRI3 (late phase). All detected brain regions that received direct projections from the hippocampus were of particular interest.
2. To strengthen the informational value of the study, I also investigated whether the above-mentioned effects can be inverted by exposing hippocampal neurons to the conflicting condition of chronic inhibition (hM4D group). Successful reversal of the adaptive process would presumably lead to an initial decrease in glutamate levels and volume increase during MRI3.
3. The changes in GMV of the hM3D group are said to be accompanied by initially increased levels (MRS 2) of glutamate / glutamine (surrogate of neuronal activity), followed by a subsequent decrease (MRS 3) and altered levels of N-acetylaspartylglutamic acid (NAA / NAAG, marker of neuronal integrity) and taurine (marker of astroglia) in the hippocampus.
4. An additional experiment was designed based on the unexpected findings of GMV changes in the main olfactory bulb (MOB) following unilateral injection. A retrograde virus was injected unilaterally into the MOB aiming to corroborate the previous observations and to visualise potential direct projections to the hippocampus.

2. Materials and Methods

2.1 Animals

Adult male C57BL/6N were bred at the animal facility of Max Plank Institute of Biochemistry in Martinsried and used for this experiment at the age of six to nine months. Animals were relocated to the animal facility of Max Planck Institute of Psychiatry and housed in individually ventilated cages (Tecniplast, IVC Green Line, Hohenpeißenberg, Germany) under standard housing conditions (23°C ± 4°C and 50% humidity ± 10%) in groups of three to five animals. All cages were standardized equipped with bedding and nesting materials, wooden enrichment tubes and *ad libitum* access to water and food. Since the treatment was administered via drinking water, water bottles (CLASSIC, crystal de-luxe mini drinking bottle, 75ml mice) were used to increase accuracy and minimise wastage of treatment. Behavioural testing and MRI procedures took place during the light phase of the circadian rhythm (light on: 07:00 am to 07:00 pm). All animal studies were conducted in accordance with the recommendations of the Federation for Laboratory Animal Science Associations and were approved by the government of Upper Bavaria.

2.2 Chemogenetic Tools

Designer receptors exclusively activated by designer drugs (DREADDs) are genetically modified human muscarinic receptors, which are used as research tool to selectivity modulate neuronal excitability. The chemogenetic variants can cell-type specific activate or inhibit neurons by using the physiological function of human G-protein-coupled muscarinic receptors (GPCRs). Membrane-bound GPCRs detect molecular ligands outside the cell and, depending on the receptor subtype, activate specific intracellular pathways. DREADDs maintain their receptor basic properties but are characteristically no longer responsive to their physiological ligand. They can only be activated by the pharmacologically inert ligand clozapine-N-oxide (CNO). The DREADD variant hM3D is a modulated excitatory receptor and

possesses the ability to enhance neuronal firing via the $G_{\alpha q}$ pathway. The activation of hM4D on the contrary, leads to a decrease in neuronal firing and synaptic silencing via the $G_{\alpha i}$ pathway (Armbruster et al. 2007). In this study, an adeno-associated virus (AAV) served as viral vector. Selective expression was obtained by using Ca^{2+}/calmodulin-dependent protein kinase (CamKII) as a cell type-specific promoter for principle (i.e. excitatory) neurons in mice. The plasmids thus included the constructs for the AAV8 serotype, the hM3D or hM4D DREADD transgenes and the transfer plasmid for the fluorescent tag mCherry under the control of the CamKII promotor. Control mice were injected with a viral construct that only carried eGFP as a fluorophore and the CamKII promotor.

2.2.1 CNO Administration

The chronic treatment of mice was initiated by supplementing drinking water with CNO (Cat. No. 4936, Tocris Bioscience, Bristol, UK). First, I daily measured the water consumption of the mice over a period of one week, to calculate the average water intake. The resulting volume consumed was about 5 ml per mouse (approx. 30 g) on average. By dissolving 0,03 mg CNO in 1 ml drinking water, a final concentration of 5 mg/kg CNO per day was achieved. The dose was chosen based on previous experiments and literature (Jendryka et al. 2019). Water bottles were light-protected, and CNO-containing solution was exchanged entirely by an interval of 60 h latest, to prevent precipitation. Following five consecutive days of chronic treatment, mice were exposed to regular drinking water for 48 h, counteracting possible receptor desensitization. I constantly monitored animals water intake by weighing the corresponding bottle per cage.

2.3 Design of the Study

Experimentally, I used chemogenetic tools in mice to investigate the effects of chronically increased or decreased hippocampal activity on the GMV of the brain. To do so, I stereotactically injected viral constructs into the dorsal CA1 region. The expression of the inhibitory (hM4D), excitatory (hM3D) and control (ctrl) DREADD in pyramidal cells was driven by the continuous application of CNO via the drinking water. Next, I performed several

MRI scans on all mice following a precise timetable. To ensure a high degree of consistency in terms of implementation, the MRI settings (e.g., positioning of bed and cryo coil) were not changed during this study. Furthermore, all scans were performed exclusively by myself following a study specific and standardized MRI protocol to minimise repositioning artefacts. Additionally, experiments analysing general activity levels (OFT) and anxiety-like (EPM) behaviour were performed to test for possible side effects of the viral construct.

2.3.1 Cohort 1 – Virus Titration

For the first experimental group, eight C57BL/6N mice were used to identify a suitable concentration of all three viral constructs. Different concentrations of the AAV8-CamKII-hM4D-mCherry ($2{,}64 \times 10^9$ gc/µl, 1×10^9 gc/µl or 5×10^8 gc/µl), AAV8-CamKII-hM3D-mCherry (3.77×10^9 gc/µl, 1×10^9 gc/µl or 5×10^8 gc/µl) and AAV2/5-CamKII-eGFP (5×10^9 gc/µl or 1×10^9 gc/µl) viruses were bilaterally injected into the dorsal CA1 region of the hippocampus. After two weeks, mice were sacrificed, and all brains removed. Brains were then cut into 30 µm thick slides using a vibratome and microscopically analysed in terms of spread and signal strength.

2.3.2 Cohort 2 – Unilateral Hippocampal Injection

The second experimental cohort was divided into three subgroups, named after the type of viral construct (hM3D, hM4D or ctrl) used. Twelve C57B/L6 mice were randomly assigned to every group, each receiving a unilateral injection of the corresponding AAV at a concentration of 1×10^9 gc/µl into the right dorsal CA1 region. After the invasive administration of the construct, mice were given a recovery and incubation time of three weeks, to ensure full expression of the DREADD. After that, the baseline scan (MRI1 and MRS1) was performed and the chronic CNO treatment initiated at a concentration of 5 mg/kg body weight. The second scan (MRI2 / MRS2) was conducted after one week (early phase) and a third scan (MRI3 / MRS3) after four weeks (late phase) of chronic activation. Between the last two scans, behavioural tests were performed. Animals were sacrificed after MRI3 and all brains collected for further histological analyses.

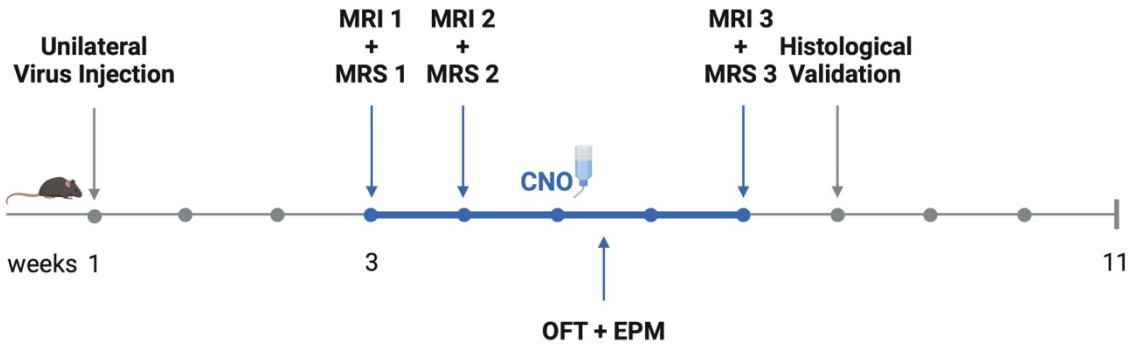

Figure 3: Schematic Representation of the Experimental Set-up for Cohort 2. Mice were injected unilaterally into the right dorsal hippocampus with the corresponding AAVs. After recovery time, three MRI scans and behaviour tests were performed according to the presented timetable. All brains were later collected for further histological analyses. (Illustration created using BioRender.com)

2.3.3 Cohort 3 – Bilateral Hippocampal Injection

In accordance with cohort 2, 36 C57BL/6N mice were again randomly assigned to three groups, this time receiving a bilateral injection of the corresponding viral construct into the dorsal CA1 region. Again, after a three-week recovery, a baseline scan (MRI1) was performed and CNO administered, followed by a second scan (MRI2) – equivalent to MRI3 of cohort 2. To examine the direct effects of chronic activation on the animals´ olfactory senses and social behaviour, a social interaction task (SIT1) was conducted. CNO treatment was then terminated, marking the beginning of a washout phase of two weeks duration. To analyse the consistency of the changes, the social interaction task (SIT2) as well as the MRI scan (MRI3) were repeated.

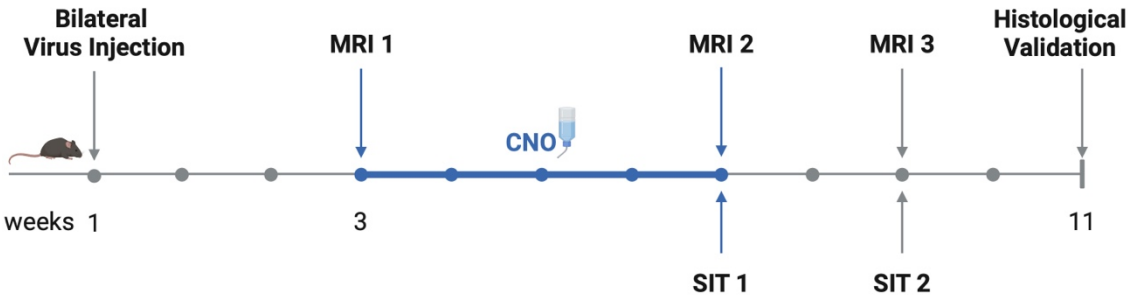

Figure 4: Schematic Representation of the Experimental Set-up for Cohort 3. All animals were bilaterally injected into the dorsal hippocampus. This time, three MRI scans and behaviour tests (SIT) were performed according to a modified timetable: after performing the baseline scan (MRI1), chronic treatment was started. After four weeks, MRI2 (comparable to MRI3 in cohort 2) was conducted and treatment was stopped. MRI3 and SIT 2 were conducted after a washout phase of two weeks; the duration of the entire experiment was extended to 11 weeks. All brains were collected and stored for further histological analyses. (Illustration created using BioRender.com)

2.3.4 Cohort 4 – Retrograde Tracing

Four C57BL/6N mice were injected unilaterally into the right olfactory bulb using 100nl of fluorogold (Fluorochrome LLC, Denver, Colorado USA), a retrograde tracer. All animals were sacrificed after one week and all brains collected for further histological analyses.

2.4 Intrahippocampal AAV Vector Injection

Animals were given 200 mg/kg of metamizole and 5 mg/kg of metacam subcutaneously 10 minutes before being anesthetized with a mixture of isoflurane (Isofluran CP®, cp-pharma®, Burgdorf, Germany) and medical oxygen (0,5 % Oxygen at a flow rate of 1.5 l/min). During the entire procedure, mice were positioned on a heating pad (approx. 35,5 °C). The animals breathing was monitored throughout the surgery and the amount of isoflurane administered (2 - 4 % for induction, 2 % for maintenance) regulated accordingly. After checking for extinguished reflexes, the head was placed into the stereotaxic frame, where nose and ear bars were adapted individually. Thereafter Bepanthen ophthalmic ointment (Bepanthen® Bayer AG, Leverkusen, Germany) was applied on the eyes to keep them moisturized during surgery. After disinfecting and locally anaesthetizing the skin with Xylocaine spray (100 mg/pump containing 10 mg lidocaine), an incision was made along the midline. A sterile cotton swab was used to remove the periosteum and 1 % H_2O_2 was applied to disinfect the exposed skull and clean it from organic material. To validate the straightness of the heads` position within the frame, the injection cannula (Neuros Syringe 5 µl, Hamilton Company) was moved along the midline of the cranium. The dorsal-ventral coordinate differences (< 0.1 mm) of Bregma and Lambda was determined and the position, if exceeding a difference of more than 0.1 mm, corrected. Subsequently, the exact coordinates of Lambda for virus injection were calculated by adding the predetermined coordinates (right side: AP: +2.3 / ML: +1,65 / DV: +1,6; left side: AP: -2.3 / ML: +1,65 / DV: +1,6) to the individual values. A small hole was then carefully drilled at the marked position. Before injecting the AAV, a small test drop was ejected to ensure proper functioning of the syringe. After positioning the needle accordingly to the calculated coordinates, 300 nl of the virus were administered at a speed of 100 nl/min using a micro injector pump. The type of virus was adapted according to the experimental subgroup assigned to the animal. After three minutes, the amount of virus injected was noted down and, in case that volume was missing, applied manually. After retraction, the skull was disinfected and the skin sutured. To accommodate the waking process, cages were partially

placed on a heating plate (approx. 36 °C) and mice were monitored until full awakening.

2.5 In Vivo Magnetic Resonance Imaging

All anatomical MR images were acquired at 9.4 T on a Bruker 94/20 Biospec system (Bruker BioSpin, Rheinstetten, Germany) equipped with a two-channel cryogenic transmitting and receiving RF coil. Animals were sedated using isoflurane, administered at a concentration of 2-4 % for induction and 2 % for maintenance, along with an airflow of 1.5 litres per minute. It then was fixated stereotactically on an animal bed in prone position and sited on a heating pad (Haake S 5P, Thermo Fisher Scientific, Waltham, United States). Its vital parameters were monitored during the scanning procedure (total time approx. 100 minutes) using a respiratory pillow (targeted respiration rate of 80-100 bpm, regulated by depth of anaesthesia) and a rectal probe (maintained at approx. 37 °C) and its eyes covered with Bepanthen ointment (Bepanthen® Bayer AG, Leverkusen, Germany). Paravision (Paravision 6.0.1, Bruker, Ettlingen, Germany) was used to acquire imaging and spectroscopic MR data. The localizer thereby marked the start of the protocol with the coil´s impedance, being individually adapted for each scan.

2.5.1 Magnetic Resonance Spectroscopy

For localization, 2D T2*-weighted structural images were acquired along all three orientations with several 30-40 slices (slice thickness 0.25 mm, no gap, image matrix = 384 x 384 voxel, repetition time (TR) = 328 msec, echo time (TE) = 3.2 msec, flip angle = 30 °, field of view (FOV) = 20 x 20 mm^2). The reference power was adjusted on a horizontal slice covering the dorsal hippocampus (region of interest for the MRS). Optimal shimming was achieved by adjusting the field homogeneity based on the B0-Map (field of view = 29 mm). Subsequent, the line width of the water signal was checked to evaluate the voxel´s shim quality. In case it met the criteria of < 20 Hz at full width at 50 % signal height and < 50 Hz at 10 % signal height, the PRESS spectroscopy (TR = 5000 msec, TE = 16.5 msec, 128 averages, voxel size = 2.50 x 1.32 x 1.52 mm^3, bandwidth = 11 ppm) was run for the right

and left hippocampus, using VAPOR water suppression. BRUKER eddy current compensation and drift correction was used. The acquisition time for each voxel was 10 min 40 sec.

2.5.2 Volumetric Analysis

In case of cohort 2, the already collected T2*-weighted structural images were used to reset the reference power (slice thickness = 1mm) to the top of the ventricles. Given that the experimental scheme for cohort 3 does not include MRS measurements, 2D T2*-weighted structural images had to be collected separately. Last, for VBM studies, anatomical images were recorded using a 3D gradient echo sequence (TR = 34.1 msec, TE = 6.25 msec, flip angle = 30 °, matrix dimensions = 256 x 166 x 205, FOV = 19.8 x 12.8 x 15.8 mm^2, isotropic pixel resolution = 77 µm).

After the scan was successfully completed, anaesthesia was faded out and mice were placed back into their cages and monitored until full recovery. The total time under anaesthesia for animals of cohort 2 amounted up to approx. 01:45 h and for animals of cohort 3 up to 01:00 h. Images were further processed and analysed as described in Chapter 2.8.Data analysis

2.6 Behavioural Testing

All behavioural tests were performed in the experimental rooms inside the holding facility of the Max-Planck Institute of Psychiatry in Munich. The experiments were set up in three detached observational areas, where each area was shielded by black walls and curtains. Three animals were transported to the experimental room and tested simultaneously. Set ups were cleaned with water containing detergent (Lisofan soap) and dried with paper towels after each animal. The following experiments were performed under low light conditions (< 20 lux) in the light phase of the animals. Videos were taped, and analyses performed using AnyMaze (4.99, Stoelting CO., USA).

2.6.1 Open Field Test (OFT)

To investigate the anxiety-like and exploratory behaviour, mice were exposed to the open field test (OFT). After placing one mouse into a corner of an empty

(50 cm x 50 cm x 50 cm) arena, facing the wall, it was allowed to explore the arena for 15 minutes. For analysis, the arena was virtually divided evenly into a rim and centre zone, using AnyMaze. Furthermore, the following parameters were detected: time in the zones, distance travelled in the zones and latency until first entry into the centre zone. Total distance moved was analysed in 5-minute-bins. Risk assessment (stretch attend posture, SAP) and rearing were analysed by an experimenter blind to the experimental conditions.

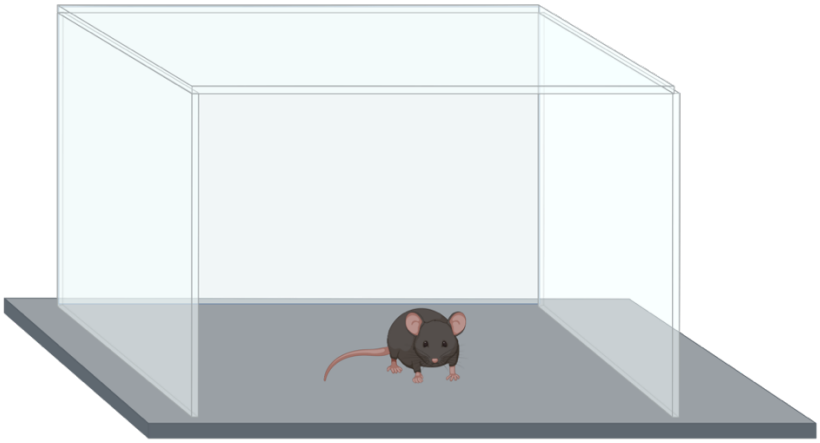

Figure 5: The Open Field Test. The open square arena was virtually divided into a rim and a centre zone. Mice are allowed to freely explore the arena for 15 min while being recorded by an overhead camera. (Illustration created using BioRender.com)

2.6.2 Elevated Plus Maze (EPM)

The Elevated Plus Maze (EPM) consists of four arms (L 27.5 x W 6 cm) perpendicularly connected by a central area (L6 x W6 cm), that is shaped like a Plus-sign and is elevated 30.5 cm above the ground. Two opposing arms are additionally equipped with 14.5 cm high walls and are therefore defined as closed arms. The remaining opposing arms are referred to as open arms as they are only bordered by a small rim, 0.5 cm high. To start the experiment, mice were place into the closed arms facing the end wall. They were allowed to explore the apparatus freely for 15 minutes. The following parameters were detected: time and distance travelled in the arms, latency to first open arm entry, total distance travelled, manual scoring of SAP, rearing and head dipping events.

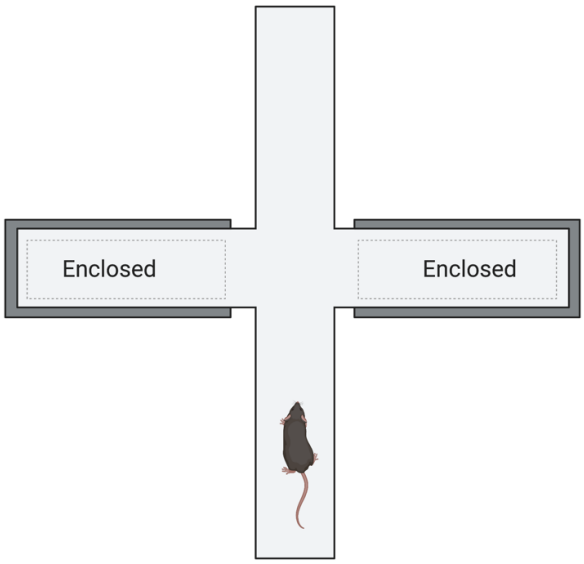

Figure 6: The Elevated Plus Maze. The elevated, plus-shaped arena consists of two oppositely positioned opened arms, two oppositely positioned closed arms and a centre zone. Mice can freely explore the apparatus for 15 minutes while being recorded by a camera placed above the maze. (Illustration created using BioRender.com)

2.6.3 Social Interaction Task

Experimental mouse was placed into the middle chamber (10 x 25 cm) of a rectangular three chamber box, that is connected to a left and right chamber (20 x 25 cm). The floor of the arena was covered with litter to simulate an accustomed environment and renewed after each trail. Chambers can be separated by using the gate-controlled middle sections of the middle chamber. Two identical pencil cups with metal wire, that allowed fresh air flow but no direct physical contact, were placed into the left and right chamber. In the first stage, mouse was able to freely explore all chambers for 10 minutes. Then mouse was placed back into the neutral chamber. A never-before-met mouse (stimulus 1) was placed in one container, whereas a neutral stimulus (glass object) was displayed in the other. Mouse was again given 10 minutes to freely explore. The placement of the stimulus in either the left or right chamber was altered between trails. Again, mouse was placed back into the middle chamber. For the third stage, the neutral stimulus was replaced by another never-before-met mouse, serving as a new stimulus. Throughout the entire experiment mice were tracked and recorded using Anymaze. Videos were recorded for further behavioural analysis.

Figure 7: The Social Interaction Task (SIT) The three-chambered-box has openings between all chambers, with two chambers being equipped with empty pencil cups. The mouse faces 3 phases of 10 min each, in which it is confronted with either no (1st stage), one (2nd stage) or two stimuli (3rd stage). An overhead camera is used to record the mouse. (Illustration created using BioRender.com)

2.7 Histological Analysis

If not stated otherwise, all animals were deeply anaesthetized with an overdose of Isoflurane and decapitated. The brains were carefully separated from the scull and snap frozen in methyl butane. Tissues were then stored at - 80 °C for further analysis.

2.7.1 Perfusion

Mice of cohort 1, 3 and 4 as well as three of cohort 2 were deeply anaesthetized with an overdose of isoflurane and transcardially perfused with ice-cold PBS followed by 4 % paraformaldehyd (PFA) solution. The brains were carefully removed and post-fixed in 4 % PFA for 24 h, cryoprotected in 20 % sucrose solution for at least 48 h and later stored at 4 °C until sectioning.

2.7.2 Histological Validation of Viral Constructs

Three perfused brains of each subgroup in cohort 2 and cohort 3 were randomly selected for sectioning. Brains were cut into 40 µm thick slices using a vibratome (HM650v, Microm, Walldorf, Germany). Slices of all brain regions were collected and placed in PBS. The free-floating slices were placed on microscopic slides to perform immunofluorescence microscopy on. Pictures were taken on microscope slides and were used to validate the spreading and expression of the virus. All slides were analysed using the Axioplan 2 imaging microscope (Zeiss, Oberkochen, Germany) and pictures were captured using a microscopic camera (Axiocam MRm 1.4MP Monochrome CCD, Zeiss, Oberkochen, Germany) and 5 x, 10 x and 20 x lenses (Plan-Neofluar objective lens, Zeiss Oberkochen, Germany). Images were processed using the image processing software Fiji (http://ImageJ.net; version 2.1.0/1.53c, 2020).

2.7.3 Immunohistochemistry (IHC)

A second series of the brain slides used in 2.7.2 for validation of the hM3D group in cohort 2 were used for IHC. The free-floating slices were washed three times in PBS for 10 min. Overnight, slices were placed into the primary solution, containing the 1st antibody (rabbit anti-mcherry antibody #ab167453 (abcam)), diluted 1:500 in PBS supplemented with 1 % NGS and 0.3 % Triton. The day after, slices were washed three times in PBS for 5 min before being placed into the secondary solution, consisting of the 2nd antibody (goat anti-chicken secondary antibody Alexa 594 #A11042, 1:1000 PBS with 1 % NGS, 0,3 % Triton) for 2 hours. Finally, slices were again washed in PBS for another 3 x 5 min and presented on microscope slides. All steps were conducted at room temperature and slices were protected from intense light irradiation.

2.7.4 Histological Evaluation of Retrograde Tracing

Brains from cohort 4 were perfused as described in 2.7.1 and equally processed as described in 2.7.2.. Pictures taken during the immunofluorescence microscopy were then analysed and edited using the image processing software Fiji.

2.8 Data analysis

2.8.1 Analysis of MRS Data

Spectral analysis and estimation of metabolic concentrations were conducted using LCModel 6.3 (s-provencher.com/lcmodel.shtml). I used the 9.4T basis spectra provided in LCModel and an analysis widow ranging from 4.3 - 0.2 ppm. All MRS data were normalized to total H_2O concentration.

2.8.2 Statistical Analysis of Behavioural and MRS Data

All data are presented as means ± SEM (standard error of the mean) and subsequently statistically analysed and graphically illustrated using GraphPad Prism (GraphPad Software, version 9.0.2 (134), 2021). I used one way ANOVA (analysis of variance), two-way ANOVA followed by Tukey's multiple comparison test (*$p < 0.05$, **$p < 0.01$, ***$p < 0.001$) and unpaired t-test to analyse behavioural and MRS data in terms of group differences. Statistical significance was set at $p < 0.05$.

2.8.3 Analysis of MRI Data

The rodent longitudinal toolbox (RLT, dbm.neuro.uni-jena.de) for statistical parametric mapping (SPM12) (Wellcome Department of Cognitive Neurology, London, UK, version: 7219) was used for the VBM analyse of the mouse brain. Imaging data was first converted to NIFTI format. The voxel size was then artificially rescaled by a factor of 10 to allow for optimal usage of the SPM default values for human brains. After brain extraction, DARTEL normalization was used to generate a study specific brain template. Initially the subject-specific images of all three timepoints were realigned performing a rigid body transformation and transformed to the temporal average using non-linear deformations. The grey matter tissue probability maps were then normalized and modulated with the Jacobian matrix to the template space. The individual´s flow field hereby stored the deformation information of the normalization between subject space and template space and were applied to the normalized images. Subsequently, differences between the modulated normalized images at two different time points were calculated. The modulated

differential GM images were finally smoothed using a Gaussian kernel of 5.7 mm.

Statistical analysis was performed using a full factorial design with the three-level factor “group” (hM3D, hM4D and controls). Additionally, an explicit brain mask, deriving from the DARTEL study specific template, was applied. No global normalization was used, as such effects should have been cancelled in differential images. Then, the full factorial model was run independently to compare the time points MRI2vs1 and MRI3vs1. Cluster significances were evaluated at $p < 0.005$, extend 20 and t-values within the cluster identified using the “find nearest local maximum”. The clusters peak t value was extracted in the matlab window (MathWorks, Natick, MA) by requesting the “beta” variable. Values were later converted into percentage and illustrated in graphs.

To visualise and interpret the different brain regions on the MRI scans, the structural images were compared with the best-fitting slides from the kimlab unified anatomical atlas (Chon, Vanselow, Cheng, and Kim 2019) and mapped by eye.

3. Results

3.1 Cohort 1 – Virus Titration

Mouse brains injected with viral constructs of varying concentrations were histologically analysed to determine the most effective concentration. The optimal outcomes in terms of virus spreading, expression, and signal strength versus background noise were observed at a concentration of 1 x 10^9 gc/µl. Consequently, this concentration was utilized for all subsequent unilateral and bilateral hippocampal injections.

3.2 Cohort 2 – Unilateral Hippocampal Injection

Initially each group, the hyperactivated hM3D-, the hypoactivated hM4D- and the control group, consisted of 12 mice. Body weight (see A) in Figure 8) remained stable throughout the experiment and no group differences were observed in the amount of consumed water mixed with CNO (see B) in Figure 8). One animal in the hM4D- and two in ctrl-group had to be excluded due to health reasons, leading to a decrease in water consumption in the fourth week.

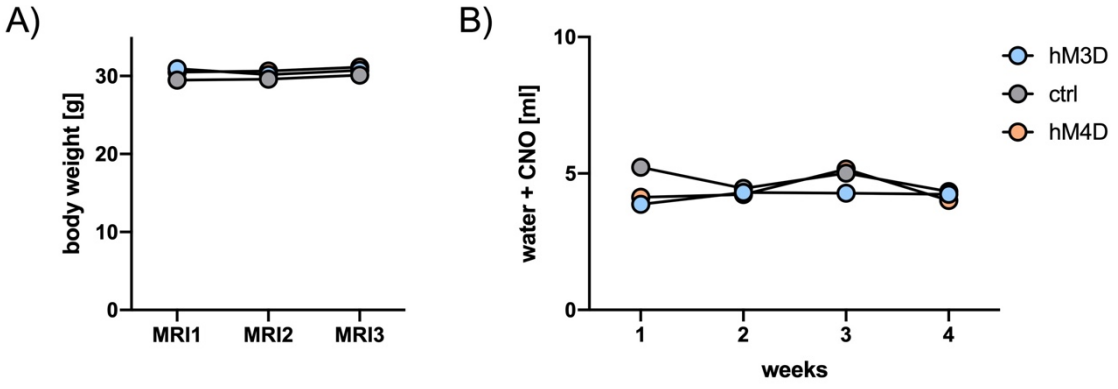

Figure 8: Consistency of Body Weight and Water Consumption. The body weight (A) and water consumption (B) of all animals in cohort 2 were measured throughout the experiment. No significant differences between the groups were detected. (One-way ANOVA followed by Tukey's multiple comparison test).

3.2.1 MRI Results – Unilateral Hippocampal Injection

3.2.1.1 Early Phase

After one week of chronic CNO treatment, resulting in DREADDs activation, the structural images from the first and second MRI scans were analysed using a voxel-based whole-brain analysis. Blue-coloured clusters indicate the brain areas where volume changes were observed. The exact volume changes, in percentage relative to the control group, are shown in the corresponding diagrams and Table 2. Volume changes were detected in the right MOB and the anterior amygdala area (AA), which partially includes the nucleus of the lateral olfactory tract (LOT) (see Table 2). The GMV of mice in the hyperactivated hM3D group slightly decreased whereas a slight increase in GMV volume was observed for the hypoactivated hM4D group compared to the control group.

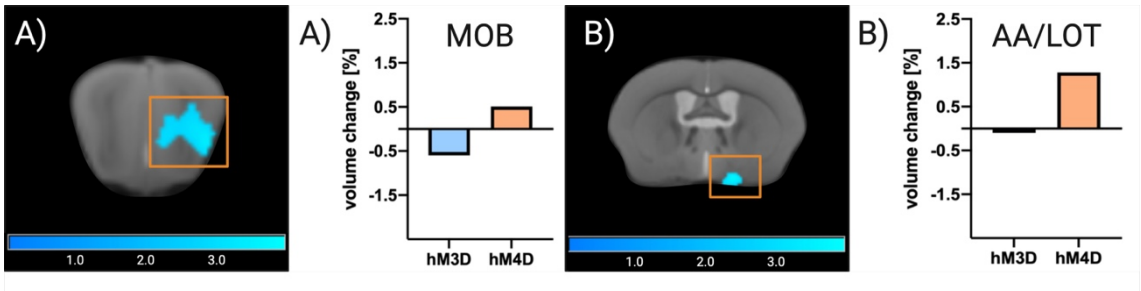

Figure 9: Longitudinal Assessment of GMV Changes in Cohort 2 after 1 Week of DREADDs Activation (MRI2vs1)l Percental brain volume changes were assessed using VBM between MRI at baseline and after one week with hM3D < hM4D (statistical map (blue) depicting two-dimensional regions with significant volume changes at a level of $p < 0.005$). Colour bar indicates t-values. The corresponding volume changes (in percentage normalized to ctrl group) are shown graphically. Volume loss was detected in all hyperactivated animals (blue bar) and volume increase in all hypoactivated animals (orange bar). The right side of the MRI image corresponds anatomically to the right hemisphere.

Table 2: Detailed Listing of Percental Volume Changes displayed in Figure 9**,** showing the cluster detected in MRI2vs1 in cohort 2.

Figure 9	abbr.	identified cluster	hM3D	hM4D
A)	MOB	main olfactory bulb	- 0.60 %	0.51 %
B)	AA / LOT	AA including LOT	- 0.10 %	1.28 %

3.2.1.2 Late Phase

The third MRI scan, performed after 4 weeks of DREADDs activation, revealed additional GMV changes in several brain regions when compared to baseline (MRI3vs1). The yellow clusters indicate those brain areas. All percental volume changes were normalized to the control group. The hyperactivated group showed a decrease in all clusters with the strongest decreases measured in the Ent, AA, subiculum and DG. In contrast, the inactivated group showed volumetric increases in all clusters with the strongest being the ENT.

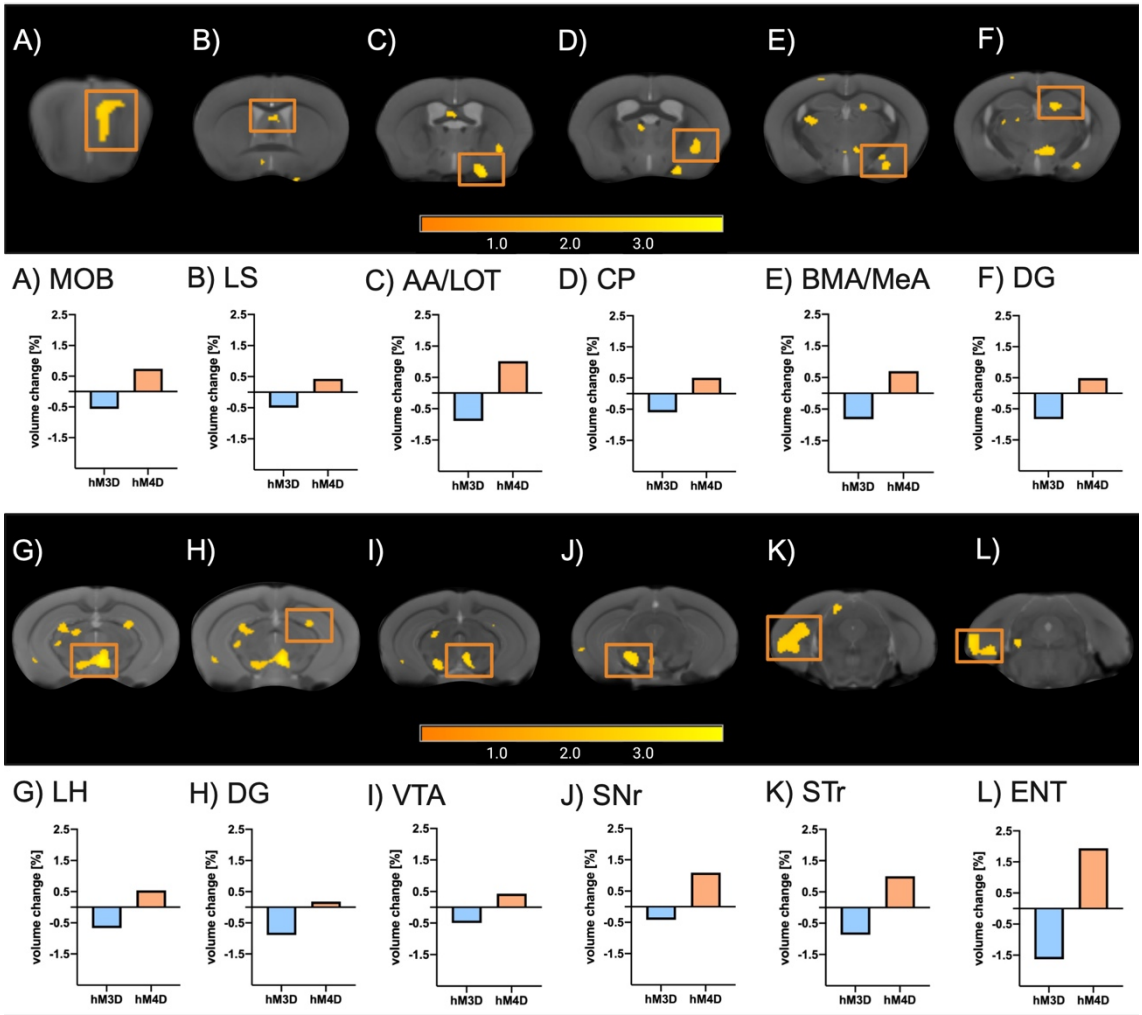

Figure 10: Longitudinal Assessment of GMV changes in Cohort 2 after 4 Weeks of DREADDs Activation (MRI3vs1). Percental brain volume changes were assessed using longitudinal VBM between MRI at baseline and after four weeks with hM3D < hM4D (statistical map (yellow) depicting two-dimensional regions with significant volume changes at a level of $p < 0.005$). Colour bar indicates t-values. The corresponding volume changes (in percentage normalized to ctrl group) are shown

graphically. Volume losses over time were detected in all regions in hyperactivated animals (blue bar) and volume increases in all hypoactivated animals (orange bar). The right side of the MRI image corresponds anatomically to the right hemisphere.

Table 3: Detailed Listing of Percental Volume Changes displayed in Figure 10, showing the cluster detected in MRI3vs1 in cohort 2.

Figure 10	abbr.	identified cluster	hM3D	hM4D
A)	MOB	main olfactory bulb	- 0.56 %	0.74 %
B)	LS	lateral septal nucleus	- 0.50 %	0.43 %
C)	AA / LOT	AA including LOT	- 0.89 %	1.02 %
D)	CP	caudoputamen	- 0.66 %	0.44 %
E)	BMA / MeA	basomedial and medial amygdaloid nucleus	- 0.82 %	0.70 %
F)	DG	dentate gyrus	- 0.83 %	0.49 %
G)	LH	lateral hypothalamus	- 0.67 %	0.54 %
H)	DG	dentate gyrus	- 0.89 %	0.18 %
I)	VTA	ventral tegmental area	- 0.67 %	0.54 %
J)	SNr	substantia nigra	- 0.42 %	1.09 %
K)	STr	subiculum transition area	- 0.87 %	1.00 %
L)	ENT	entorhinal cortex	- 1.63 %	1.94 %

3.2.2 MRS Results – Unilateral Hippocampal Injection

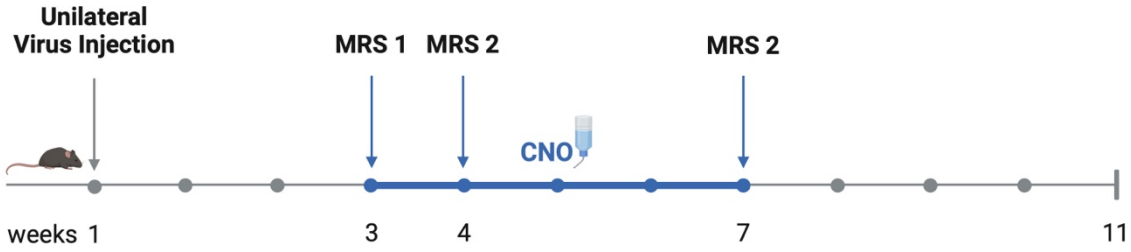

Figure 11: Timetable of MRS Measurements in Cohort 2 MRS data were acquired simultaneously with MRI1, 2, and 3, corresponding to one, two, and four weeks after DREADDs activation. (Illustration created using BioRender.com)

Magnetic Resonance Spectroscopy was conducted simultaneously with MRI 1 (naive), 2, and 3 (mice exposed to CNO) in cohort 2, with each box in Figure 12 and Figure 13 representing the MRS data at the corresponding time point. The first graph of each timepoint shows data for the right hippocampus, while the second graph presents the left hippocampus. The two most common internal references used in animal studies for normalization of MRS data are creatine (Cr) and water. Due to the inconsistency in concentration of creatinine in cohort 2 (see Figure 12) all following MRS data in Figure 13 were normalized to the voxels water content.

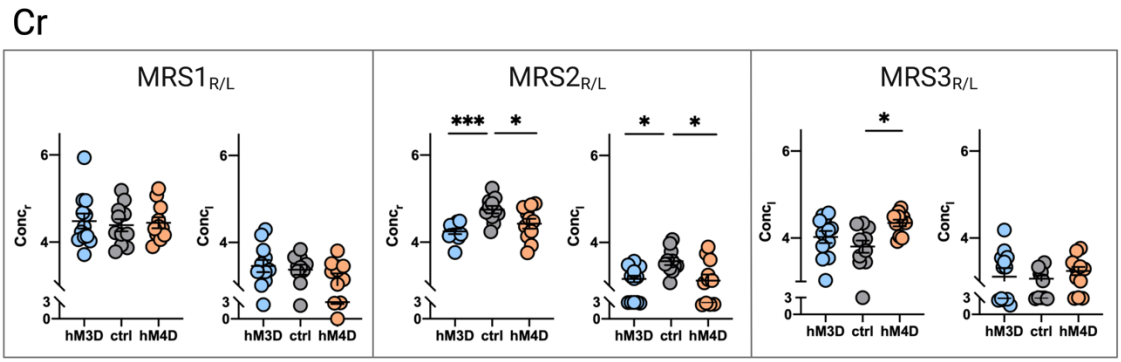

Figure 12: Significant Inconsistency in the Concentration of Creatine Measured over Time. Data was acquired over a period of four weeks. Metabolites for hM3D (blue), control (grey) and hM4D (orange) were measured for each hippocampal hemisphere individually. The first graph within the box shows MRS Data for the right hippocampus (injection site), the second graph for the left hippocampus. Concentrations [ppm] significantly differed between groups; (one-way ANOVA followed by Tukey's multiple comparison test (*p < 0.05, **p < 0.01, ***p < 0.001).

Three hippocampal metabolites and their concentration changes were of particular interest in this study. The concentration of glutamine and glutamate (Gln_Glu) as indicator of neuronal activity, NAA_NAAG as markers of neuronal integrity and taurine as marker of astroglia. At baseline (MRS 1), no significant differences were detected between the groups. But slight deviations in concentration levels were observed, notably lower on the left compared to the right side (injection site). In the second MRS, significantly lower levels of Tau were found in the right hemisphere in both experimental groups compared to the control group. The left hippocampus exhibited lower concentrations of Gln_Glu and Tau in the hM4D group, and a significantly lower concentration of NAA_NAAG in the hM3D group. Overall, no group difference between hM3D and hM4D could be detected. After four weeks of chronic treatment, all the above-mentioned effects were no longer detectable.

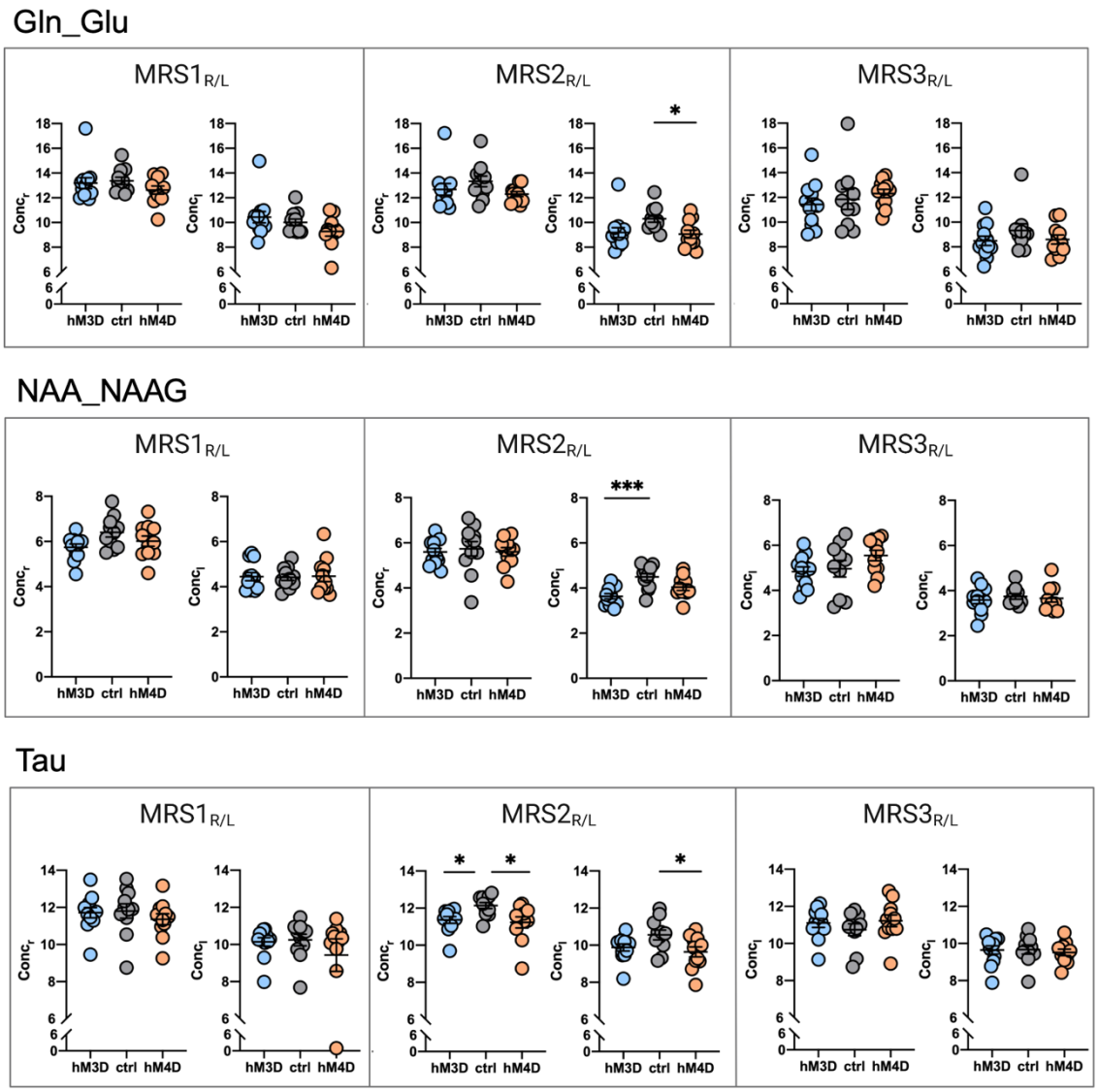

Figure 13: Longitudinal Assessment of Changes in Hippocampal Metabolites using MRS. Charts present relative concentration levels of several metabolites measured on every single timepoint (MRS1,2 or 3). Changes in metabolites in hyperactivated animals (blue), control (grey) and inactivated animals (orange) were compared for each site of the hippocampus individually. The first graph within the box represents the right site (injection site), the second one the left site (one-way ANOVA followed by Tukey's multiple comparison test (*p < 0.05, **p < 0.01, ***p < 0.001).

3.2.3 Behavioural Test Results – Unilateral Hippocampal Injection

3.2.3.1 The Open Field Test (OFT)

The OFT was conducted following 4 weeks of DREADD activation (see experimental scheme in Chapter 2.3.2). The OFT was used to determine general activity levels and locomotor activity in mice. There was a significant decrease in total distance travelled ($p = 0.046$) and in number of entries to the rim zone ($p = 0.030$) in hyperactivated compared to inactivated animals, but not when compared to the control group. No significant differences were recorded in the manual analyses of behaviour. The hM3D group only differed significantly in the latency to first entry of the centre zone when compared to the ctrl group.

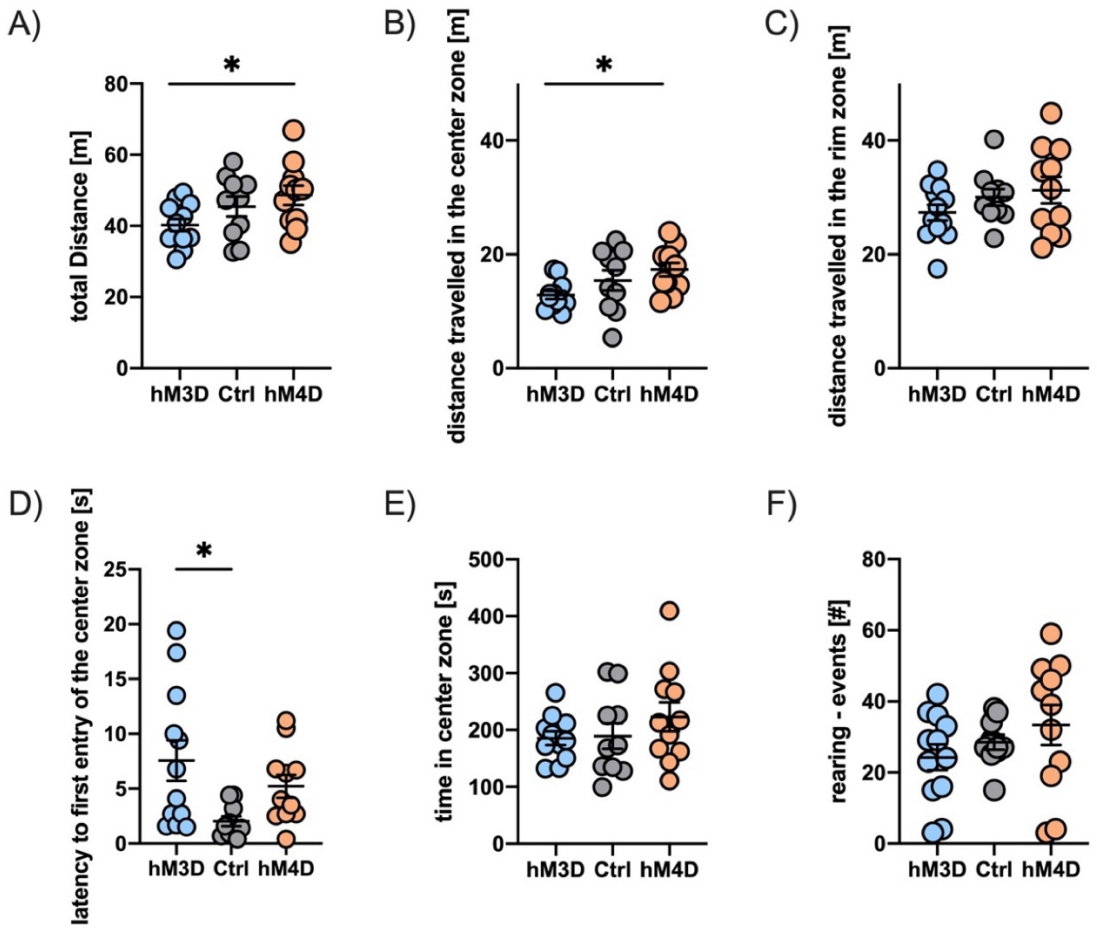

Figure 14: Open Field Test Results (Cohort 2) Animals in the hM3D group only differed significantly in the latency of first entry of the centre zone when compared to the control group. Among hM3D and hM4D, the significant differences were observed only in total distance travelled and numbers of entries to the centre zone. Data are presented as ±SEM; (one-way ANOVA followed by Tukey's multiple comparison test (*$p < 0.05$, **$p < 0.01$, ***$p < 0.001$)).

3.2.3.2 Elevated Plus Maze (EPM)

The EPM was conducted after the OFT to assess anxiety-related and explorative behaviour. Animals in the hM3D group showed a decrease in total distance travelled ($p = 0.015$) and in number of entries to the open arms ($p = 0.003$) compared to the ctrl group. The distance travelled in the closed arm was significantly lower in the hM3D when compared to the other groups. The scoring of behaviour by an unbiased experimenter showed a significant decrease in the number of rearing events (actively observing the environment while standing on hind legs) in hM3D compared to hM4D. One animal in the hM4D group fell of the apparatus and was excluded from group analysis.

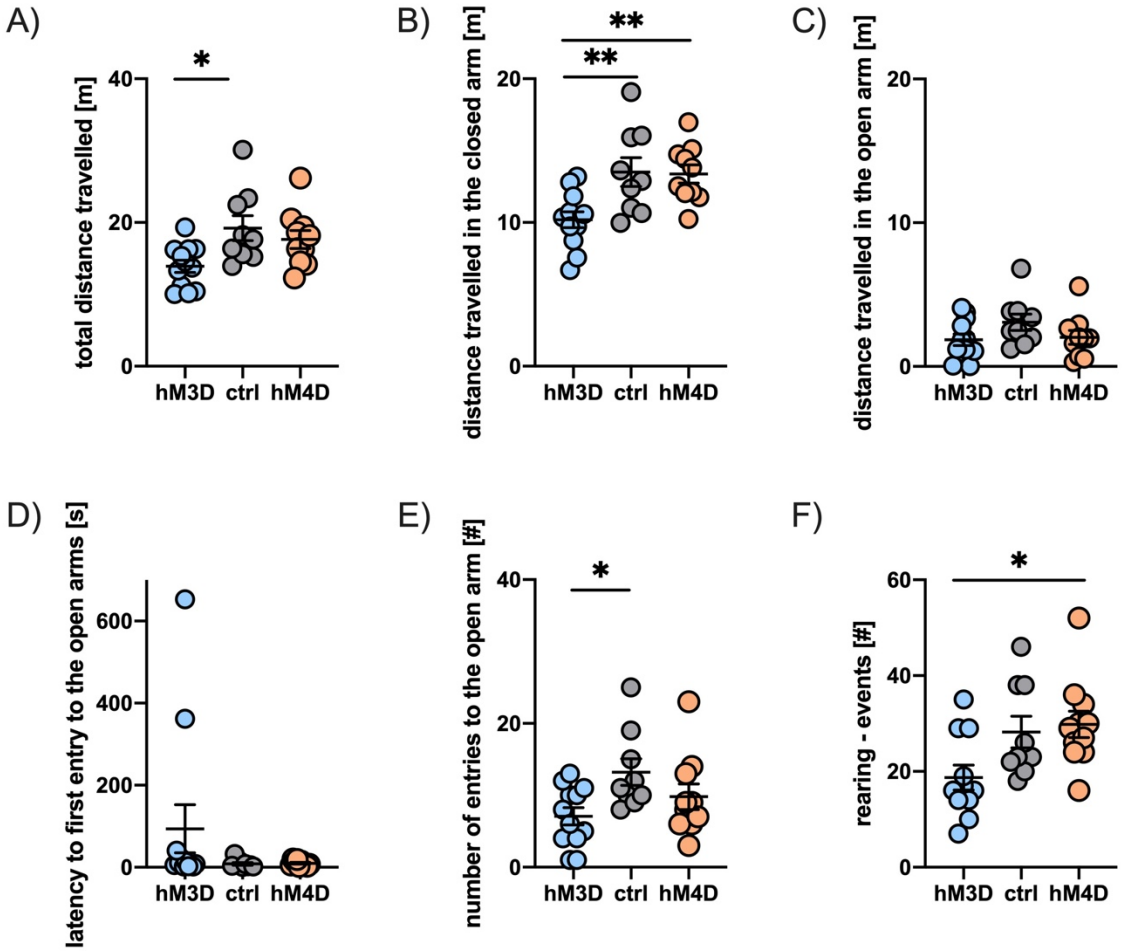

Figure 15: Elevated Plus Maze Results (Cohort 2) Hyperactivated animals (blue) significantly differed from the controls (grey) in terms of total distance travelled and number of entries to the open arm. Intervention groups differed in number of rearing events and distance travelled in the closed arm. Data are presented as ±SEM, *significantly different; (one-way ANOVA followed by Tukey's multiple comparison test (*$p < 0.05$, **$p < 0.01$, ***$p < 0.001$)).

3.2.4 Histological Validation – Unilateral Hippocampal Injection

The validation of injection sites was conducted using the structural MR images as shown in the first column in Figure 16. All histological images presented in this study were processed for saturation and contrast. The expression of the AAV8-CamKII-hM3D-mCherry (B) - D)) and AAV8-CamKII-hM4D-mCherry (F) - H)) was mainly detectable in the dorsal CA1 field and more precisely in the pyramidal layer of the hippocampus. The AAV2/5-CamKII-eGFP (J) - L)) showed a more widespread expression across the entire hippocampus, especially the DG.

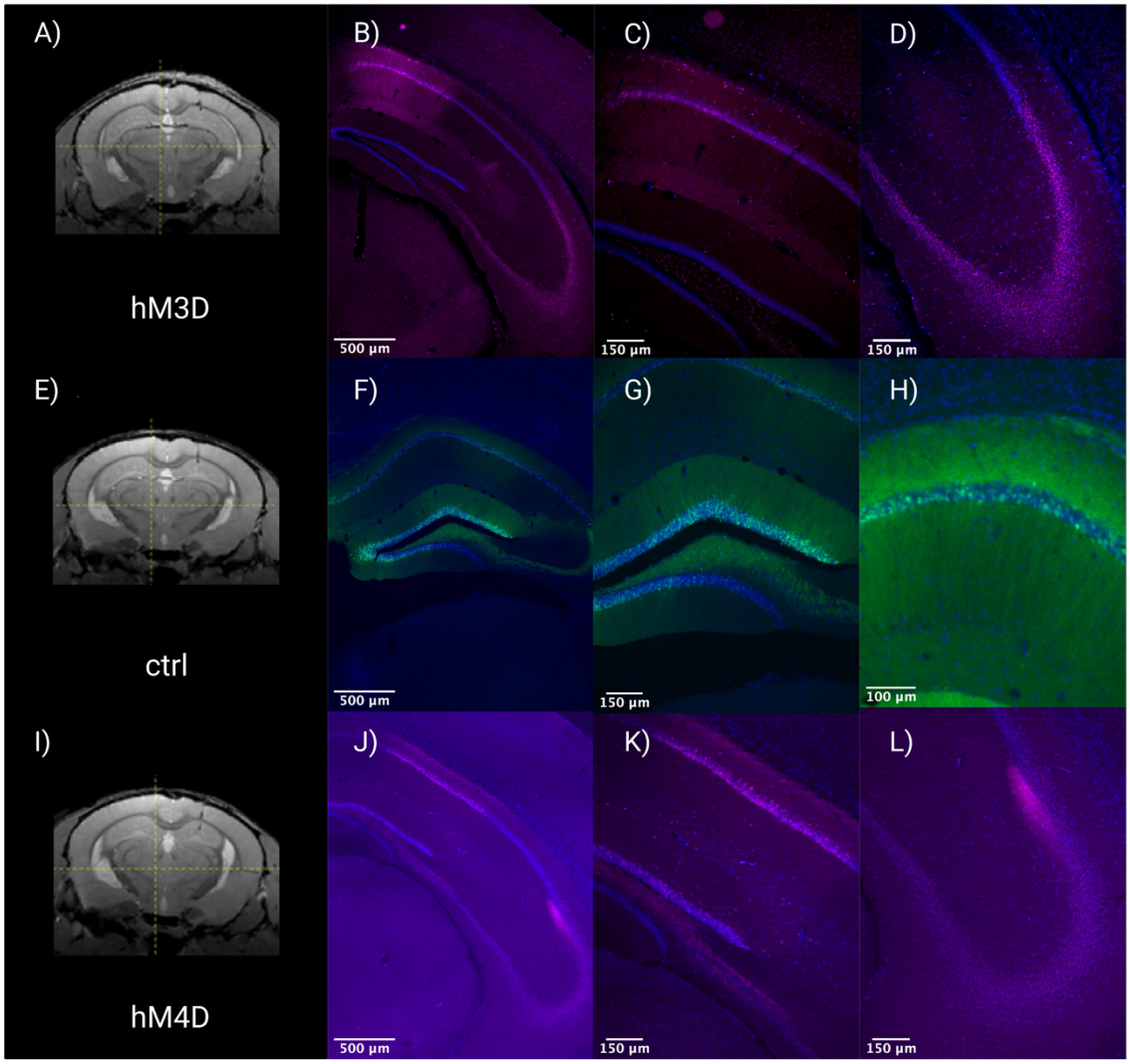

Figure 16: Validation of Injection Sites and Virus Expression in Cohort 2 using MRI and Histological Images. Structural MRI images are presented in the first column to validate the injection site. The following three histological images evidenced the expression and spreading of the virus: hM3D **(A – D)** and hM4D **(I – L)** show detection of fluorescence signal in the pyramidal cell layer of dorsal and ventral CA1; ctrl **(E – H)**:

widespread signal throughout the hippocampal formation; Presented images have been processed for saturation and contrast.

Fluorescence signals were also detected in the MOB of mice in the hM3D- (A - C) as well as hM4D- group (D - E) after unilateral injection (see Figure 17).

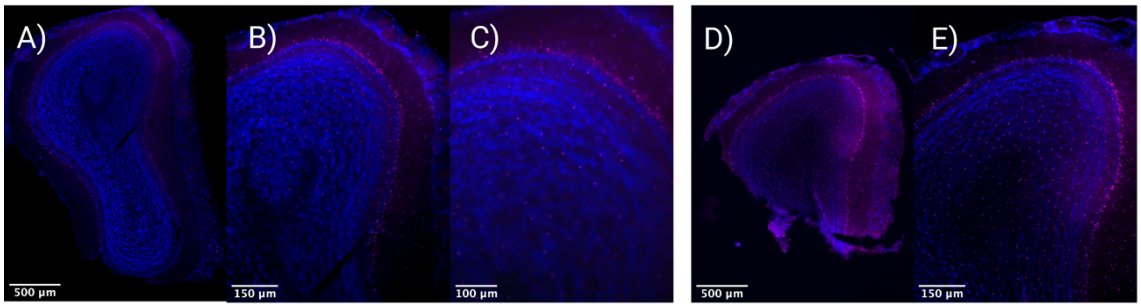

Figure 17: Histological Images of Cohort 2 Showing Projections to the MOB hM3D **(A – C)** and hM4D **(D – E)** show fluorescence signals in the MOB recorded in cohort 2 after unilateral injection of AAV into the dorsal CA1 region; presented images were processed for saturation and contrast.

3.2.5 Immunohistochemistry of the Viral Construct "hM3D"

An immunohistochemical staining was additionally conducted to refine the analysis of the AAV8-CamKII-hM3D-mCherry. The hippocampus depicts strong fluorescence signals in the CA1 region with clearly recognisable staining of single pyramidal neurons (see C) in Figure 18).

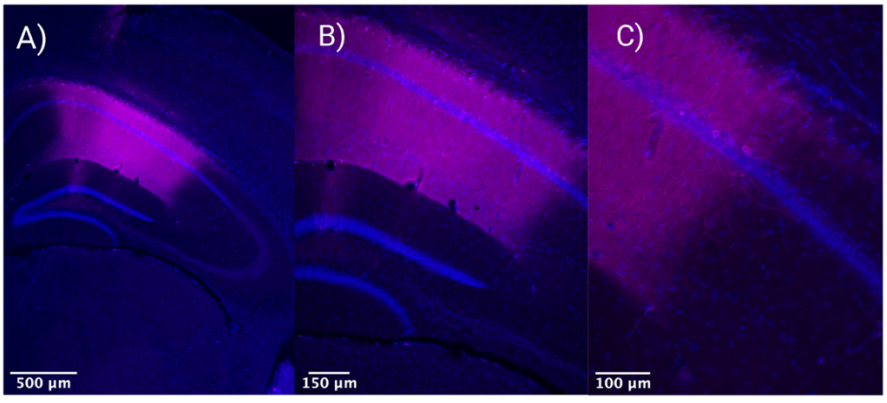

Figure 18: Second Histological Analyses of Viral Construct Expression in the hM3D Group. A) B) and C) show strong fluorescence signals in the CA1 region of the right hippocamps. C) depicts 3 pyramidal cells. Presented images have been processed for saturation and contrast.

3.3 Cohort 3 – Bilateral Hippocampal Injection

Initially each group, the hyperactivated hM3D-, the hypoactivated hM4D- and the control group, consisted of 12 mice. One mouse in the hM3D group had to be excluded due to health reasons. Body weight of all mice remained stable throughout the experiment and no group differences were observed in the amount of consumed water blended with CNO.

3.3.1 MRI Result – Bilateral Hippocampal Injection

After 4 weeks of chronic treatment and DREADDs activation, the second MRI scans were compared to the baseline (MRS2vs1). Yellow-coloured clusters indicate the brain areas where volume changes were observed. The exact volume changes, in percentage relative to the control group, are shown in the corresponding diagrams. The identified clusters included the primary somatosensory cortex, SNr and interpeduncular nuclei. The hM3D group showed volume loss in all and the hM4D group volume increase in all but one cluster when compared to the control group. In cohort 3, different brain areas are identified compared to the pattern of volume change observed after unilateral hippocampal injection in cohort 2 (see Figure 10).

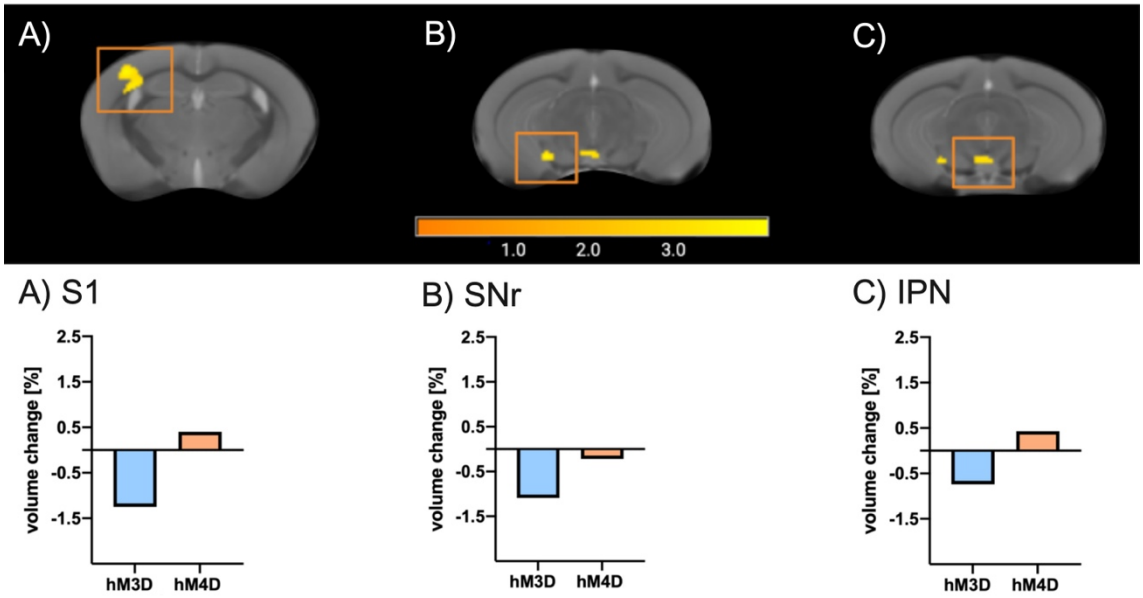

Figure 19: Longitudinal Assessment of GMV Changes in Cohort 3 after 4 Weeks of DREADDs Activation (MRI2vs1). Percental brain volume changes were assessed using longitudinal VBM between MRI at baseline and after four weeks with hM3D < hM4D (statistical map (yellow) depicting regions with significant volume changes at a level of $p < 0.005$). Colour bar indicates t-values. The corresponding

volume changes (in percentage normalized to ctrl group) are shown graphically. Volume losses over time were detected in hyperactivated animals (blue) and volume increases in all but one region for hypoactivated animals (orange). The right side of the MRI image corresponds anatomically to the right hemisphere.

Table 4: Detailed Listing of Percental Volume Changes displayed in Figure 19, showing the cluster detected in MRI2vs1 in cohort 3 – Bilateral Injection.

Figure 19	abbr.	identified cluster	hM3D	hM4D
A)	S1	primary somatosensory cortex	- 1.25 %	0.40 %
B)	SNr	substantia nigra	- 1.09 %	- 0.22 %
C)	IPN	interpeduncular nuclei	- 0.74 %	0.43 %

3.3.2 Social Interaction Tasks

After identifying strong discrepancies in the MRI data analysis between mice that received unilateral (cohort 2) versus bilateral (cohort 3) hippocampal injections, further evaluation of the trials was not considered useful and thus not conducted.

3.3.3 Histological Validation – Bilateral Hippocampal Injection

The initial validation of injection sites was conducted using structural MRI images (see first column in Figure 20). Additionally, two animals from each group were randomly selected to histologically analyse the corresponding viral constructs. The AAV8-CamKII-hM3D-mCherry (A) – D)) was expressed in the dorsal subiculum (dSub), but only sparsely expressed in pyramidal cells of the hippocampal CA1 region with no detectable projections to the ventral CA1. Likewise did the expression pattern of AAV8-CamKII-hM4D-mCherry (E) – H)) deviate as it was detected in the granular cell layer of the dentate gyrus, the dSub and pyramidal layer of the hippocampal CA3 region but not in the CA1 region. Only the AAV2/5-CamKII-eGFP (I) – L)) showed a comparable virus distribution to cohort 2.

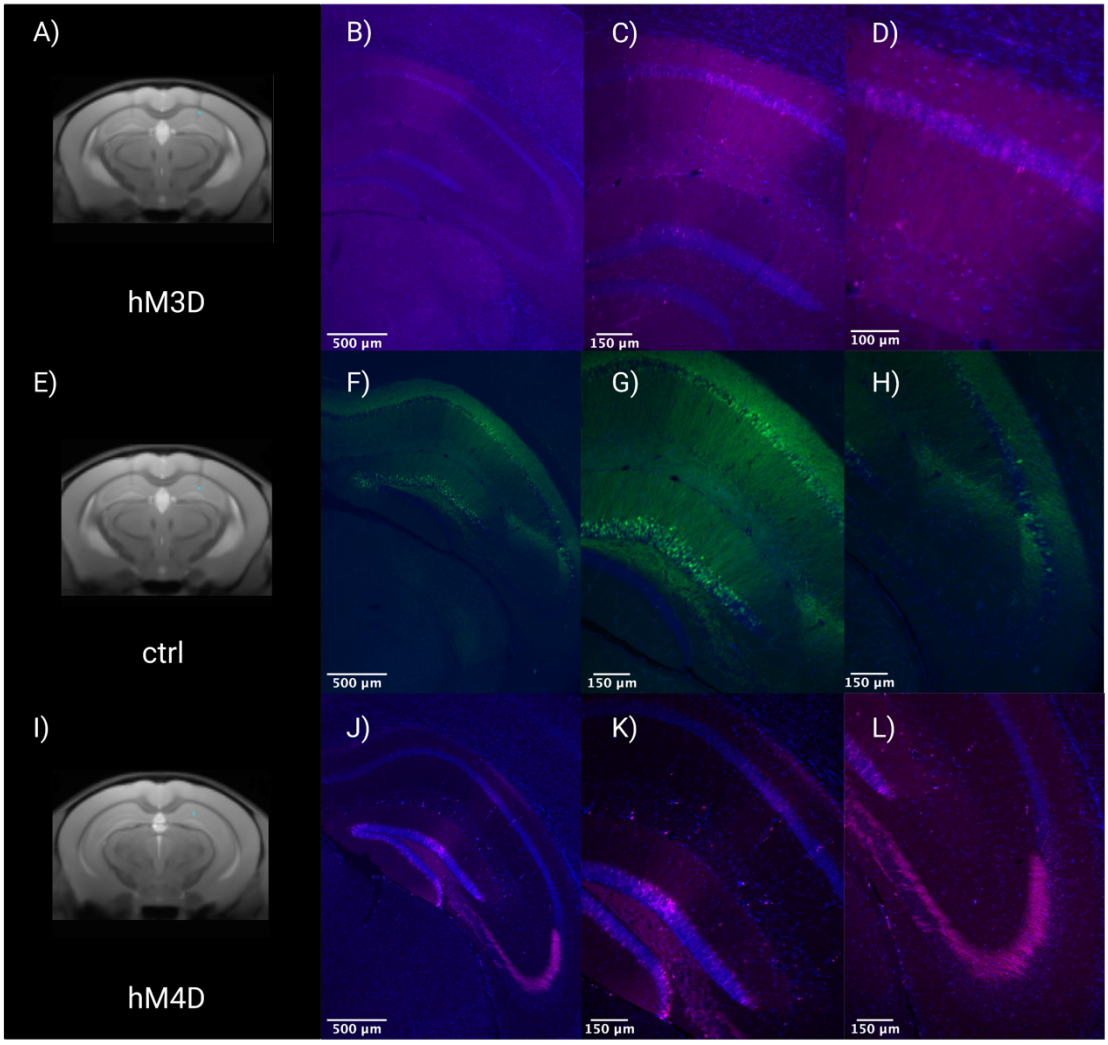

Figure 20: Validation of Injection Sites and Virus Expression in Cohort 3 using MRI and Histological Images. Structural MRI images are presented in the first row to validate the injection site. The following three histological images display the expression of the virus**:** **A - D)** hM3D: weak fluorescence signal in CA1 of hyperactivated mice; **I - L)** hM4D: signal detected in the dSub, DG and CA3; **E - H)** ctrl: widespread signal throughout the hippocampal formation; Presented images have been processed for saturation and contrast.

3.4 Cohort 4 – Retrograde Tracing

The MRI analysis of mice unilaterally injected into the hippocampus revealed volumetric changes in the main olfactory bulb (see A) in Figure 10). To investigate the presence of direct hippocampal projections to the MOB, Flurogold was used as a retrograde tracer. In addition to the commonly described direct projections to the piriform cortex and cortical amygdala, direct projections to the ventral CA1 were detected in this study.

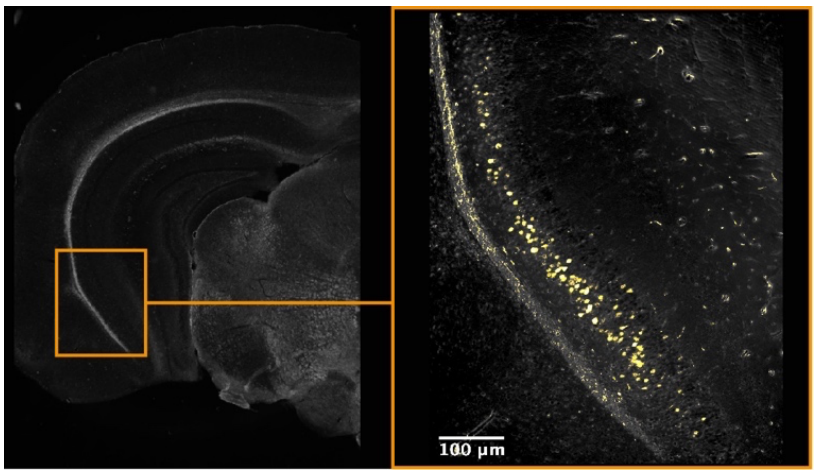

Figure 21: Histological Images showing Direct Projections found in the Ventral CA1 Region after Injecting a Retrograde Tracer into the MOB. The first image displays the left hippocampus using a DAPI filter (Alan Brain Atlas Picture 81). On the right, an enlarged view of the CA1 region is shown, highlighting nuclei labelled by FluoroGold as a result of retrograde labelling of the projection site. The images have been processed for saturation and contrast.

4. Discussion

Schizophrenia is ranked among the top 25 leading causes of disability worldwide, with a mean life-time prevalence of 1 %. Patients are at high risk for social descend and a variety of comorbidities, resulting in a potential life loss of 13-15 years (Hjorthøj, Stürup, McGrath, and Nordentoft 2017; Lu et al. 2022).

But despite intense research, the causes and the underlying pathophysiological mechanism of schizophrenia remain unknown. Recent neuroimaging studies however managed to detect a precise pattern of morphological brain changes in the hippocampus that correlate with the onset of schizophrenia. Accordingly, the disease pattern in the prodromal stage shows hypermetabolism first in the hippocampal CA1 region and later in associated regions of the hippocampus. This coincides with an initial increase in grey matter volume which turns into a reduction at later stages (Lieberman et al. 2018; McHugo et al. 2018; Schobel et al. 2013). The causal relationship between increased neuronal activity and biphasic changes in grey matter, however, remains to be demonstrated.

Therefore, the aim of my thesis was to study the consequences of chronically increased or decreased neuronal activity at the level of the hippocampal CA1 region on changes in grey matter volume. I therefore used a combination of chemogenetic tools and longitudinal MRI measurements in mice. Based on VBM analyses, animals exposed to increased neuronal firing in the hM3D group showed a loss of volume, while neuronal inactivation in the hM4D group seemed to cause an increase in volume. Despite the limitations of this study, the presented trend supports the idea of chronic neuronal overstimulation being a potential driver of GMV losses in schizophrenic patients as advocated by several other studies (Lieberman et al. 2018; Schobel et al. 2013; Haukvik et al. 2015; Ho et al. 2017; Small et al. 2011).

4.1 Volumetric Changes and Homeostatic Plasticity

Monitoring changes in the brain structure over time has become an increasingly important research tool in the field of psychiatry. It allows the detection of yet undiscovered affected regions and the investigation of potential pathophysiological mechanisms. There are invasive (e.g., histological analyses of brain slides, two-photon microscopy) and non-invasive (e.g., MRI and MRS) methods available to examine and measure structural changes. In-vivo MRI hereby exhibits substantive advantages. It allows scientists to repeatedly monitor changes over time without influencing the observed mechanism itself. Also, one can acquire big data about the whole brain while detecting even small changes. The voxel-based morphometry (VBM) used in this study is a highly suitable, unbiased, and quantitative way of analysing differences between grey and white matter distribution for each voxel over time.

Mice of a similar age exhibit physiological, age-dependent changes in GMV across various brain regions (Asan et al. 2021). To account for these age-related effects, the study's volumetric analyses were normalized to the control group. Consequently, the graphs in Figure 9 and Figure 10 exclusively display the volumetric changes induced by the specific viral constructs used in each experimental group. Mice in the hM3D group were exposed to chronically increased neuronal firing of pyramidal neurons, while those in the hM4D group experienced silencing of hippocampal neurons. As hypothesized, I was able to detect contrary alterations in GMV volume in response to both stimuli. According to the findings of this study, increased neuronal activity in the hippocampus was followed by expending GMV losses in all efferent structures over time. In contrary, the reduction in neuronal activity was accompanied by an increase in volume in analogous structures.

4.1.1 Early Volumetric Changes secondary to Increased Neuronal Activity

The activation of the neuronal network triggers a wide range of processes within the brain. Pyramidal neurons in the hippocampus are a type of excitatory neurons. When neuronal activity levels are high, pyramidal neurons initially increase their firing frequency and additionally fire action potential using their dendrites, a phenomenon known as *dendrites spiking* (Holthoff, Kovalchuk,

and Konnerth 2006). In highly active neurons, the increased influx of calcium ions activates a variety of cellular processes such as the transcription of the brain-derived neurotrophic factor (BDNF) (Miranda, Morici, Zanoni, and Bekinschtein 2019). BDNF has neuroprotective properties and provokes an increase in the number, size and complexity of dendrites. It therefore facilitates the physiological adjustments required to adapt to the elevated demands. It also strengthens synapses and increases cell differentiation and improves survival. Furthermore, the neurophysiological process of *synaptic plasticity* enables neurons to adapt to the current level of activation. High-frequency bursting of hippocampal neurons thereby triggers the anti-homeostatic process of long-term potentiation (LTP) (Hobbiss, Ramiro-Cortés, and Israely 2018; Stampanoni Bassi et al. 2019). LTP is an activity-dependent and NMDA-mediated process, that leads to the strengthening of synapses. It is input-specific, hence it only releases chemical messengers and activates NMDA receptor on the receiving and previously activated neuron. This causes the remodelling of dendritic spines and increases the volume, stability, and clustering of spines. LTP also leads to an elevation in neuronal excitability, which in turn raises the probability for further LTPs to be initiated. All the adaptations of cellular mechanisms change the brain volume of the respective area. Increases in dendritic spine density, for example, elevate VBM signalling and are associated with GMV increase (Keifer et al. 2015).

I therefore expected to observe an increase in GMV (MRI2) and in glutamate levels (MRS2) after one week of elevated neuronal activity in the hM3D group of cohort 2. But volumetric changes detected in MRI2 already indicate a slight volume loss in the hM3D group, while mice exposed to a decreased level of neuronal activity (hM4D) showed an increase in volume (see Figure 9). Also, no increase in glutamate levels was detected in the hM3D group (see Figure 13).

Along with the general limitations of this study (see Chapter 4.5), the timing of MRI2 and MRS2 requires critical evaluation. Conducting MRI2 one week after construct activation may have been too late, possibly missing early morphological changes. As a result, MRI2 likely captured a more advanced stage of volumetric changes, potentially leaving early alterations undetected.

4.1.2 Late Volumetric Changes secondary to Increased Neuronal Activity

A moderately and time-limited increase in neurotransmitter release in the hippocampus leads to overstimulation of postsynaptic neurons and can cause psychotic and cognitive symptoms. Constantly high levels of glutamate, however, induce cellular stress on neurons. Stress and hyperexcitation, for example, accelerate the depletion of neuronal stem cells (Sierra et al. 2015) and reduces the concentration of protective neurotrophic factors (Banasr, Sanacora, and Esterlis 2021). This leads to a reduction in neuroprotective capacity and an increased neuronal vulnerability. After a disproportionately long activation phase, neurons will therefore have to protect themselves from overexcitation and neurotoxicity (Newcomer, Farber, and Olney 2000). In experimental studies, exposing mice to chronic stress induced dendritic reorganisation, reduction in number of synapses, neuronal atrophy, and synaptic loss (Radley et al. 2004; Wellman 2001). Persistently high levels of glutamate, for instance, are found in the hippocampus during the early stages of schizophrenia (Schobel et al. 2013). Using MRS to detect these early changes, however, is challenging and leads to inconsistent findings in literature. In early stages, some studies observe increasing concentrations (Duarte and Xin 2019), while others report stable or decreasing trends (R.S. Kahn and Sommer 2015). This variability in glutamate levels across different brain regions reflects the complexity of glutamatergic dysfunction in schizophrenia. In late stages, however, studies tend to show a more consistent pattern of decreasing glutamate concentrations (Duarte and Xin 2019; R.S. Kahn and Sommer 2015). For NAA / NAAG on the other hand, a continuous decrease in concentration is reported (Duarte and Xin 2019; R.S. Kahn and Sommer 2015).

I therefore hypothesised that after four weeks of DREADDs activation, MRI 3 would capture volume reduction in hyperactivated animals of the hM3D group. In MRS 3, I expected decreased glutamate levels in the hM3D group compared to the hM4D group.

The analysis of MRI 3 revealed volume reduction in several brain areas following neuronal hyperactivation (see Figure 10). Reversing the effect by inactivating pyramidal neurons in the hM4D group, led to a volume increase in efferent structure. The MRS results in this study (see Figure 13), however, did

not show a consistent picture that fits the described pathophysiology. Technical inaccuracies like water suppression or the small sample size along with high variances may have obscured such subtle changes in metabolites. Considering other imaging methods like the 2-Photon-microscopy or cellular analysis (e.g., golgi staining or western plots) may therefore provide a more detailed and accurate picture of underlying cellular mechanism.

4.2 GMV Changes associated with Cognitive and Negative Symptoms

In MRI3, the strongest percental volume changes were observed in the highly interconnected hippocampal formation itself and the brain regions that receive direct hippocampal projections:

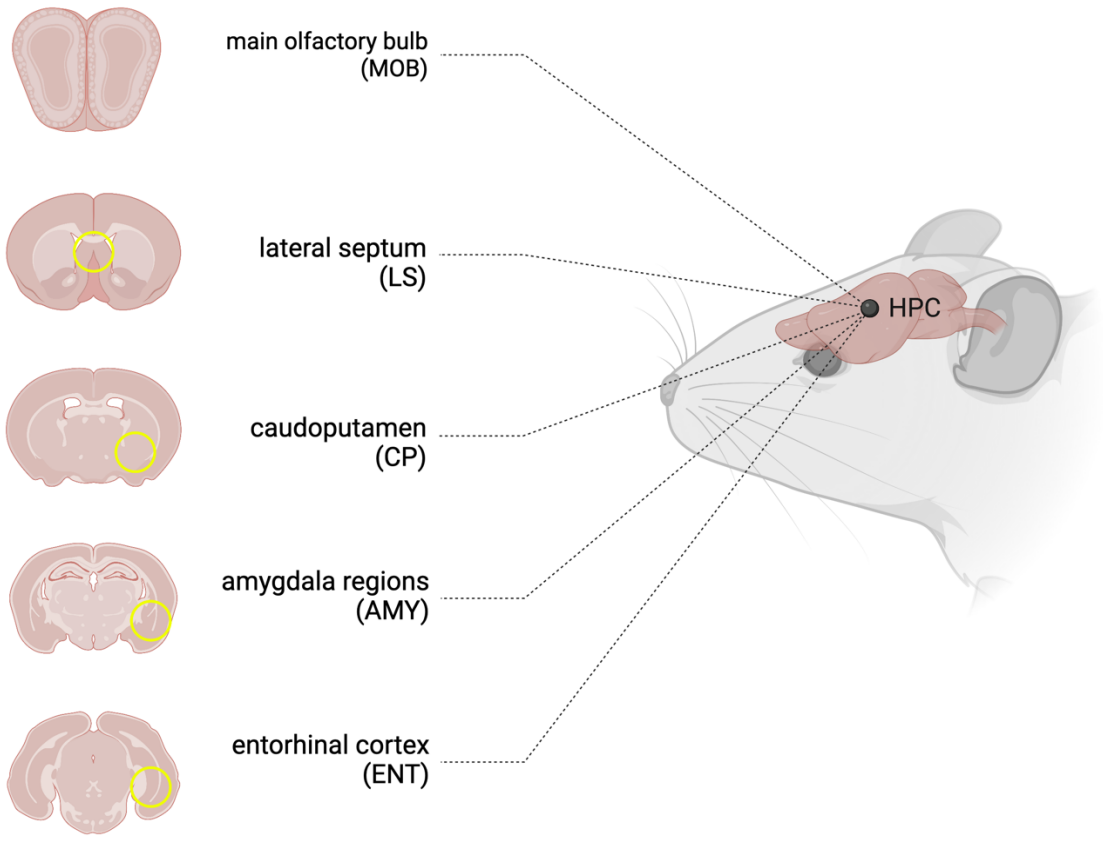

Figure 22: Illustration of known Direct Hippocampal Projections to Brain Areas detected in this Study. The hippocampal formation (HPC), including the subiculum, possesses direct connections to the entorhinal cortex (ENT), amygdala regions (AMY), caudoputamen (CP), lateral septum (LS) and the main olfactory bulb (MOB). (Illustration created using BioRender.com)

4.2.1 The Entorhinal Cortex

In the hM3D group, the increasing excitatory neurotransmitter release in the CA1 region entailed a non-regulated overstimulation of efferent postsynaptic neurons. The ENT, which has strong direct, bilateral, and bidirectional projections to and from the CA1 region and subiculum, is significantly influenced by hippocampal hyperactivation. Fittingly, the strongest volumetric changes in this study were detected in the ENT (see Figure 10). The affected ENT transmits the altered neuronal activity to all components of the hippocampus, with the strongest influence on the dentate gyrus (DG) (Fanselow and Dong 2010; van Groen, Miettinen, and Kadish 2003). Stronger volumetric changes were also observed within the subiculum, which is the main output region of the hippocampus and direct target of CA1 and the DG. As observed in the hM3D group, overstimulation of the hippocampus resulted in a loss of volume, indicating hippocampal dysfunction. With no proper hippocampal functioning, however, processes like memory consolidation, gating of declarative memory and primary cognitive function (dorsal part) or regulation of stress response, emotion and affects (ventral part), can no longer be precisely modulated (Haukvik et al. 2015; McDonald and Mott 2017; Nakahara, Matsumoto, and van Erp 2018; Small et al. 2011). Hippocampal malfunctioning is therefore associated with negative and cognitive symptoms in patients with schizophrenia. Unfortunately, measuring metabolites related to neurotransmission (see Figure 13) could not provide any further information about the subtle dynamic changes within the hippocampal formation.

4.2.2 The Amygdala-Nucleus Region

In addition to the volumetric changes observed in the hippocampus, the study also detected changes in the GMV of the amygdala nucleus region. This region includes the AA and LOT as well as in the BMA and MeA. These findings seem reasonable, as both represent key components of the limbic system and share massive bidirectional connectivity. The interconnection between the amygdala and the hippocampus is essential for memory consolidation. It facilitates neuronal plasticity and synaptic interaction by synchronizing the firing of pyramidal neurons (Ahnaou et al. 2020; McDonald and Mott 2017). Especially the ventral CA1 and subiculum send and receive direct projections from all

three detected amygdala regions (see Figure 10). The MeA hereby shares bidirectional connections with the intermediate CA1 and subiculum (Fanselow and Dong 2010). These linking properties substantiate the dependence of amygdala regions on proper hippocampal functioning and their sensitivity to altered electrical inputs. As seen in hM3D group, increased excitatory neurotransmitter release in the hippocampus is accompanied by volume reduction in the amygdala regions. The amygdala regions are therefore strongly affected by the hippocampal hyperactivation. The resulting disruption of the amygdala contributes to negative and cognitive impairments in schizophrenic patients. It negatively influences their behaviour, as the amygdala controls many complex brain functions. For instance, it is significantly involved in processing of fearful and rewarding stimuli, fear conditioning or extinction, anxiety-like behaviour, and memory consolidation in terms of emotional events (Janak and Tye 2015). To do so, the amygdala receives and processes information from many different brain regions, including all sensory modalities.

4.2.3 The Main Olfactory Bulb

Noteworthy, volume reduction was also observed in the MOB. The MOB is a highly plastic structure capable of continuous neurogenesis that has direct contact to the outside world. It also is the only sensory system that does not rely on thalamic circuits to process sensory information. The olfactory sensory neurons register odorants and project via the mitral cells to the glomeruli, the first olfactory structure that interacts with the central nervous system. The responsiveness and activity of the human olfactory network can be modulated by higher processing areas in the brain. Depending on the processing areas, the network can be divided into three categories: the *sensory network* processes basic olfactory impressions while the *frontal network* integrates olfactory information at a higher level. The *limbic network* includes the anterior and posterior hippocampus as well as amygdala and relays emotional and homeostatic information (T.C. Arnold et al. 2020). Upon closer examination, the unexpected volumetric alterations in the MOB, seem to be explicable. The integration of primary sensory information in humans has evolved over the course of mammalian evolution (Bergmann, Zur, Bershadsky, and Kahn 2016). In humans, hippocampal connections were

rerouted via the association cortices to allow for more abstract stimulus representation and cognitive processes (Bergmann, Zur, Bershadsky, and Kahn 2016; I. Kahn et al. 2008; Zhou et al. 2021). In rodents however, the hippocampal network preserved their connections to the primary sensory cortices. Importantly, regarding the findings of this study, the rerouting processes were only reported for visual, auditory, and somatosensory inputs but not for the olfactory system. Hence, direct projections and resting functional connectivity between the hippocampus and primary olfactory cortex still exist in humans. The human olfactory-hippocampal network has thus been preserved and corresponds to that of rodents (Zhou et al. 2021). The hippocampus can therefore directly influence the proper functioning of the MOB, as pyramidal cells in the ventral CA1 and ENT send direct projections to the granule cell layer of the MOB (Huart, Rombaux, and Hummel 2013; Padmanabhan et al. 2018). Interestingly, schizophrenic patients can present with olfactory disfunction (Moberg et al. 1999). Volume size hereby correlates positively with functionality (Huart, Rombaux, and Hummel 2013; Moberg et al. 2014). Both findings of this study, the structural changes in the MOB (see Figure 9 and Figure 10) and the histological proof of direct projections in mice (see Figure 21) support the idea of hippocampal dysfunction being the driving force. Furthermore, the ventral CA1 does not only project to amygdala regions and the MOB, but to all cortical areas that directly receive olfactory inputs (e.g., piriform area, anterior olfactory nucleus, LOT). In addition, the MeA and BMA both receive strong inputs from the main and accessory olfactory bulb and are involved in sociosexual behaviour (MeA) or integration of olfactory information (BMA).

Although still rare, studies on olfactory dysfunction in schizophrenia hold significant potential. There are different tests available to determine the level of smell dysfunction. The odour threshold test, for example, assesses the peripheral olfactory function. The discrimination tests provide information about executive functions (working memory) and, together with the identification test, about cognitive functions (semantic memory). Patients with schizophrenia show impairment in all olfactory testing. Patients with frontal temporal dementia, on the other hand, show impairment only in the odour identification test

(Carnemolla et al. 2020). Therefore, olfactory tests may serve as supportive diagnostic tools in the future, as they can help to differentiate between different psychiatric and neurodegenerative diseases.

4.3 GMV Changes associated with Positive Symptoms

Schizophrenic patients, that experience positive symptoms like hallucinations or delusions, process and interpret external stimuli misleadingly. They no longer react appropriately to their environment, as they lose their ability to differentiate between reality and perception. Some hear voices, sounds or other auditory stimuli that are not actually present or are misinterpreted stimuli. In health, the novelty detection and salience attribution processes allow the brain to prioritize information and respond adaptively to the changing demands of the environment. Multiple brain regions are involved in these complex and dynamic processes. The anterior cingulate cortex, for example, monitors incoming sensory information and assesses its significance. The subcortical dopamine systems, including the nucleus accumbens (NAc), and the ventral tegmental area (VTA), are responsible for reinforcing behaviour by incorporating the brain`s reward system.

4.3.1 The Ventral Tegmental Area

The hippocampal formation can influence novelty detection processes and salience attribution via its polysynaptic pathways to the VTA (see Figure 23). Newly identified stimuli are sent via the NAc and ventral pallidum (vP) to the VTA. This functional connectivity is used to process and compare novel stimuli and to store information. The hippocampal-VTA loop also gates the entry of information into the long-term memory stored in the hippocampus. Importantly, it permits previously stored information to be overwritten only if the newly presented information is of sufficient behavioural importance (Lisman and Grace 2005; McHugo et al. 2018).

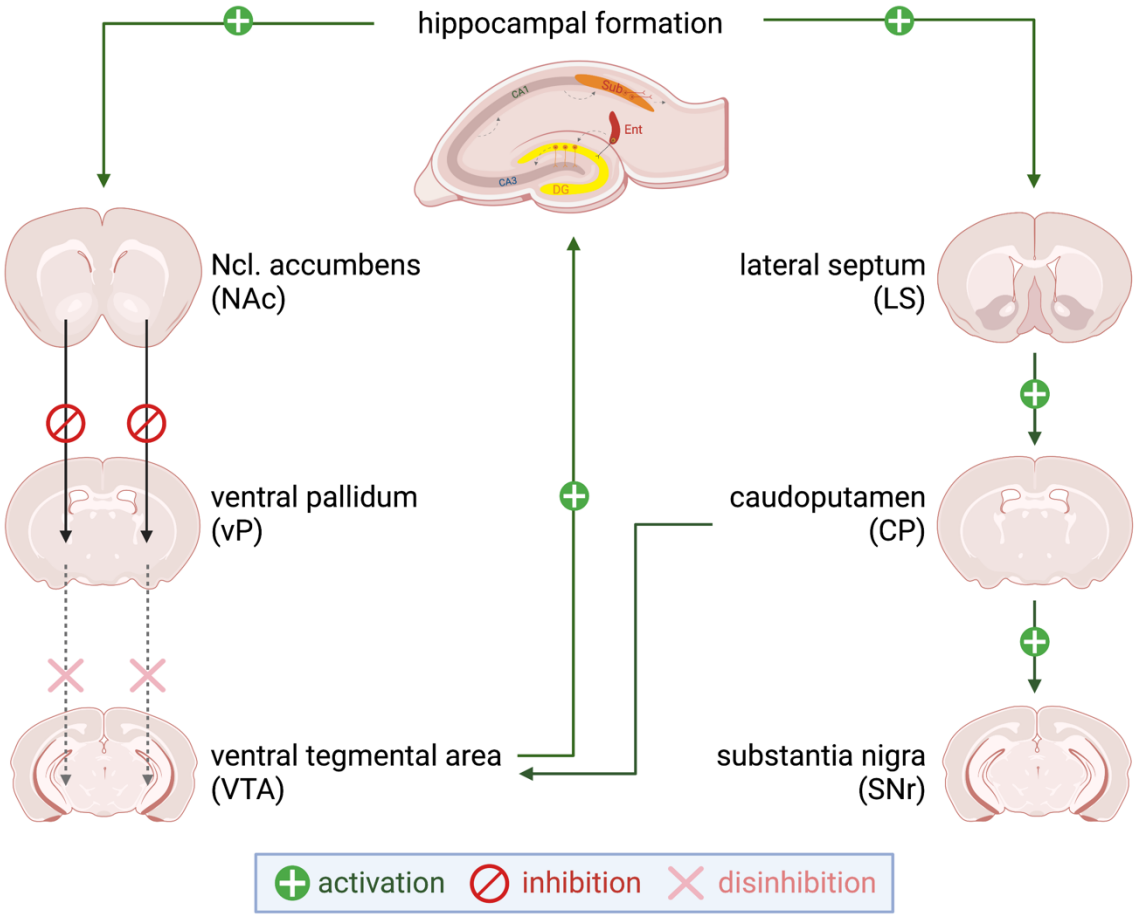

Figure 23: The Hippocampal-VTA Loop: To date, there are no direct projections known, that connect the hippocampus with the ventral tegmental area (VTA) and substantia nigra (SNr). The hippocampal CA1 region rather compares novel inputs from the ENT to direct cortical inputs and selectively passes them on to the subiculum and forward to the nucleus accumbens (NAc). The latter inhibits the ventral pallidum (vP), which normally tonically inhibits DA neurons in the VTA. The disinhibition leads to a novelty-dependent activation of the VTA. The VTA in return has strong dopaminergic projections to the ventral hippocampus itself (Lisman and Grace 2005; McHugo et al. 2018). HPC can also send signals via the LS and CP to the VTA and SNr. LS further communicates with the HPC via second-order projections (Deng et al. 2019). (Illustration created using BioRender.com)

Dopamine normally does not create salience acquisition and expression but modulates it in a stimulus-dependent manner (Kätzel, Wolff, Bygrave, and Bannerman 2020). There are two independently regulated ways of dopamine release in the striatum (including NAc and CP):

(1) The phasic spike-mediated release of dopamine is driven by dopaminergic neuron burst firing and is functionally relevant for reward prediction and incentive salience. It characteristically generates a large amplitude but short duration of firing. The phasic release cannot impact extracellular DA levels nor induce homeostatic changes.
(2) The tonic dopamine release does not require dopaminergic neuron firing. It is induced by glutamate released from cortical afferences, that act on presynaptic NMDA receptors in dopamine terminals. The NMDA-depended tonic release causes a low amplitude but slow and long-lasting release of dopamine. It can modulate extracellular dopamine concentrations. The tonic release is involved in setting the resting state level of dopamine receptor stimulation, thus system activation.

Thus, an aberrance of tonic dopamine levels can elicit homeostatic processes. It can also determine the level of dopaminergic neuron responsivity and therefore directly influence the magnitude of phasic responses to stimuli (Grace 1991; Lodge and Grace 2007).

In patients with schizophrenia, however, the subcortical dopamine systems is dysregulated, which contributes to psychotic symptoms and aberrant assignment of salience (Kätzel, Wolff, Bygrave, and Bannerman 2020). The dysregulation is said to be induced by the hyperactivated hippocampus, linking hippocampal disfunction to positive symptoms (Lodge and Grace 2007). In support, studies showed that electrical and chemical stimulation of the ventral hippocampus in rodents causes the release of dopamine in the NAc. It also elevated the number of active dopaminergic neurons in the VTA (Kätzel, Wolff, Bygrave, and Bannerman 2020; Lisman et al. 2008). Increased hippocampal activity would thus lead to an unfounded increase in population activity and dopamine release in the VTA. In result, salience is erroneously assigned to unqualified items, evoking psychotic symptoms. The brain will continue to process the deceptive information, which is now encoded

by neurotransmitter concentrations. The false perceptions that arise in the process, then make it difficult for patients to distinguish between important and unimportant stimuli (Kätzel et al. 2020).

The dorsal CA1 can also stimulate dopaminergic neurons in the VTA via its excitatory projection to the lateral septum (LS) (see Figure 23). The dorsal subiculum and lateral band of ENT strongly innervate the CP and NAc. Both in turn project, either directly or indirectly via the pallidum, to the VTA and / or SNr. There also might be several convergence points along the way that enable communication between the dorsal and ventral hippocampus. Both receive afferences from the medial septum (MS) and share a common efference, the lateral septum, and can interact via the nucleus reunions of the midline thalamus (Fanselow and Dong 2010; Kätzel, Wolff, Bygrave, and Bannerman 2020). The longitudinal MRI data set of cohort 2 revealed volume reductions in hyperactivated animals for nearly all above mentioned areas (CP, LS, VTA, SNr), supporting the extensive and profound influence of hippocampal dysfunction. Exposing mice to hippocampal silencing, on the other hand, led to an increase in volume. The findings in the two contrasting experimental groups support the idea that altered hippocampal neuronal activity is the driving force behind the GMV changes in schizophrenic patients.

4.4 Bilateral Targeting of the Hippocampus

The second longitudinal MRI study largely resembled but augmented the first study design. The aim was to replicate and increase the observed pattern of GMV changes by amplifying the effect strength using a bilateral injection into the hippocampus. Although all other variables (e.g., CNO application, MRI setup and animal age) remained unchanged, I was not able to validate the previous results. In the VBM analysis of the structural images (MRI2) acquired in the late phase (see Figure 19), a very different pattern of GMV changes was identified. The pattern showed only similarities to the GMV changes in cohort 2 in its direction of change. Given the weak predictive power of cohort 3, I decided to neglect the examination of MRI3 and the social interaction task. Also, both were performed after an additional washout period of two weeks, which reduced their significance even further.

By changing the approach to bilateral targeting, I did not manage to amplify the potential underlying effect that was observed in cohort 2. Instead, I may have activated a different, not comparable mechanism. Targeting both sides with the same concentration of viral construct may have increased cellular stress to an intolerable level, eventually leading to loss of hippocampal plasticity and functionality. Another factor, potentially influencing the outcome, may arise from DREADDs themselves. Animals in cohort 2 exhibited sufficient hippocampal virus expression when microscopically analysed (see Figure 16), whereas fluorescence signals detected in hyperactivated animals of cohort 3 appeared considerably weaker and less spread (see Figure 20). Accordingly, the data obtained from cohort 3 are not significant nor eligible for evaluating the validity of the first study. To validate the results of cohort 2, a repeated implementation of the identical study design (see Figure 3) would be required.

4.5 Critical Assessment of the Study

The aim of the study was to detect even minor changes in GMV resulting from chronically increased or decreased neuronal activity in the hippocampus. Studying the direct consequences, however, is challenging, as the hippocampus is a very complex and highly interconnected brain region. Hippocampal neurons, for example, do not project to one brain region only. They form a diversified network across the brain, which is involved in many higher-level cognitive functions. In turn, projection areas such as the amygdala often receive and integrate numerous inputs themselves. Hippocampal afferences therefore usually make up only a small portion of all afferences. As a result, the magnitude of volumetric effects was expected to be moderate. Given the small sample size of the study in addition to the small effect size, I assumed that GMV changes would be both, subtle and difficult to detect. Hence, the p-value a voxel must exceed to be considered an active cluster, was lowered to $p < 0.005$ to allow a more nuanced analysis.

During implementation, I have tried to avoid measurement errors and deviations to the best of my knowledge. However, designing a longitudinal study to monitor subtle changes over time can be difficult, as each intervention can leave its marks and potentially interfere with the outcomes. I attempted to overcome this challenge by using DREADD´s to modulate hippocampal neuronal firing. This approach only requires a one-time invasive procedure and works site-specific, without disrupting the entire brain network. Additionally, only the right site of the dorsal CA1 was injected, to ensure functional integrity of the hippocampus. The ventral hippocampus was targeted using the virus distribution along with the strong hippocampal interconnections (see Figure 16). After the invasive implementation, animals were given three weeks to fully recover and ensure full expression of the construct. Once data collection began, only methods that require as little invasive handling and interventions as possible were used. Therefore, CNO was non-invasively applicated via the drinking water. CNO is known to enter the brain and to partly convert back to clozapine (CLZ) in mice. The conversion, however, has no impact as CLZ does not activate DREADDs because it is non-specifically bound (Jendryka et al. 2019). The experimental setup aimed to minimize handling-induced chronic stress, thereby reducing the potential for unintended brain activation. Furthermore, MRI

and MRS were used to measure structural and metabolic changes over time. Both techniques are non-invasive and considered low-risk since, apart from the known risks of short-time anaesthesia, there are no known negative and long-lasting side-affects.

Despite the above-mentioned advantages, the attempt to alter neuronal activity as physiologically as possible and only as invasively as necessary, had several down-sites. The expression of DREADDs is strongly dependent on the promotor's efficacy, i.e. on the number of infected pyramidal neurons. Transfected pyramidal neurons then do increase excitability but lack the ability to elevate overall hippocampal activity on their own. This makes the presence of external inputs essential. Since the mice were held under laboratory conditions, correspondingly in an environment with rather few stimuli, the extent of activation was expected to be moderate. In addition, activating the receptors using CNO in the drinking water added to the construct's vulnerability. In this study, no group differences were detected in the amount of water consumed (see Figure 8). It therefore was assumed but not experimentally verified that mice received sufficient CNO per day. In this study, behavioural tests were used to detect potential side effects of the chemogenetic construct. In accordance with current literature (Jendryka et al. 2019), no meaningful behavioural alterations compared to controls were detected. But, as the injection was only unilateral and behavioural tests assessed at one timepoint only, the validity of the results is limited.

The chemogenetic construct used in this study therefore carried a risk of exhibiting significant variability in its performance. The experimental setup, to the best of my knowledge, has not been conducted before and should be revised and adapted prior to renewed implementation. Instead of targeting pyramidal cells in C57BL/6N mice using DREADs, it may be more efficient to alter neuronal activity via directly targeting interneurons using NMDA receptor antagonists or knock out mice. This could help restricting the influence of parameters that are difficult to control, such as virus expression, CNO uptake and presence of sufficient environmental stimuli. Additionally, it would be recommended to conduct the behavioural tests at least twice in order to enhance its informational significance. These improvements in combination with a bigger sample size could further help to elevate the low threshold that a

voxel must exceed to be considered an active cluster. This, in turn, would strongly enhance the informative value and quality of the MRI results in this study.

As a result, the presented outcomes are rather unsuitable to allow direct conclusions concerning the underlying mechanism. Instead, the study provides valuable information about the dynamic processes associated with altered neuronal activation. It appears that the observed volume changes follow a certain pattern, where overexcitation is associated with a loss while inactivation is linked to an increase in volume over time. The pattern was consistently found in all detected brain areas (see Figure 9 and Figure 10) including nine brain areas that are directly connected to the hippocampal formation. These findings are especially informative as the monosynaptic connections permit a more detailed macroscopic examination of the consequences. Interestingly, the cluster detected are also associated with the development of either negative and cognitive (see Chapter 4.2) or positive symptoms (see Chapter 4.3). The demonstrated pattern of volume loss following hippocampal overstimulation overall, supports the hyper-glutamatergic NMDA receptor hypofunctioning hypothesis in schizophrenia and illuminates the far-ranging influence of the hippocampal network. To fully understand the functional connection between hippocampal dysfunction and the development of specific morphological changes however, more imaging studies are required.

4.6 Outlook

In line with Bleuler's initial description, schizophrenia is a heterogenous group of illnesses, with patients rarely sharing the exact same pathophysiology. The hippocampal formation, however, continues to be the most reported area of overlap. Currently, researchers are emphasizing a more personalized approach to psychiatric conditions, one that considers individual risk factors and characteristics. In this context, gaining insights through MRI studies holds great potential.

This longitudinal MRI study attempted to further investigate the dynamic processes of GMV changes following altered hippocampal neuronal activity. It showed that animals exposed to increased neuronal firing over time presented with loss of volume, while hippocampal inactivation seemed to trigger an increase in volume. For a follow-up experiment, it would be interesting to transfer the identified clusters detected in mice and their pattern of change to structural images of schizophrenic patients. At its best, using brain masking of the presented MR imaging would lead to the identification of a comparable pattern in analogous human brain structures. It would be particularly interesting to investigate whether early volume changes in the main olfactory bulb are reflected by the patients' reduced ability to smell. If so, odour tests could additionally assist in the early diagnosis of schizophrenia.

The ever-increasing volume of MRI datasets, combined with advancements in machine learning, offer a promising future for research into psychiatric disorders. Machine learning can already help to anticipate the individual course of the disease and its outcome rather than that of an entire diagnostic group (Chen et al. 2022; Dwyer, Falkai, and Koutsouleris 2018). In cases of unclear diagnostic circumstances, it can also facilitate the differentiation between depression and schizophrenia (Koutsouleris et al. 2015) or bipolar and unipolar depression (Redlich et al. 2014).

Acquiring more knowledge about the dynamic processes and pathophysiology associated with schizophrenia using neuroimaging techniques thus holds the promise of enhancing early disease detection and therapy planning. This, in turn, has the potential to significantly enhance patient compliance and improve their quality of life in the future.

Bibliography

Ahnaou, A., D. Rodriguez-Manrique, S. Embrechts, R. Biermans, N. V. Manyakov, S. A. Youssef, and Whim Drinkenburg. 2020. "Aging Alters Olfactory Bulb Network Oscillations and Connectivity: Relevance for Aging-Related Neurodegeneration Studies." *Neural Plast* 2020: 1703969. https://doi.org/10.1155/2020/1703969.

Anderzhanova, E., T. Kirmeier, and C. T. Wotjak. 2017. "Animal models in psychiatric research: The RDoC system as a new framework for endophenotype-oriented translational neuroscience." *Neurobiol Stress* 7: 47-56. https://doi.org/10.1016/j.ynstr.2017.03.003.

Armbruster, B. N., X. Li, M. H. Pausch, S. Herlitze, and B. L. Roth. 2007. "Evolving the lock to fit the key to create a family of G protein-coupled receptors potently activated by an inert ligand." *Proc Natl Acad Sci U S A* 104 (12): 5163-8. https://doi.org/10.1073/pnas.0700293104.

Arnold, S. E., B. T. Hyman, G. W. Van Hoesen, and A. R. Damasio. 1991. "Some cytoarchitectural abnormalities of the entorhinal cortex in schizophrenia." *Arch Gen Psychiatry* 48 (7): 625-32. https://doi.org/10.1001/archpsyc.1991.01810310043008.

Arnold, T. C., Y. You, M. Ding, X. N. Zuo, I. de Araujo, and W. Li. 2020. "Functional Connectome Analyses Reveal the Human Olfactory Network Organization." *eNeuro* 7 (4). https://doi.org/10.1523/eneuro.0551-19.2020.

Asan, L., C. Falfán-Melgoza, C. A. Beretta, M. Sack, L. Zheng, W. Weber-Fahr, T. Kuner, and J. Knabbe. 2021. "Cellular correlates of gray matter volume changes in magnetic resonance morphometry identified by two-photon microscopy." *Sci Rep* 11 (1): 4234. https://doi.org/10.1038/s41598-021-83491-8.

Banasr, M., G. Sanacora, and I. Esterlis. 2021. "Macro- and Microscale Stress-Associated Alterations in Brain Structure: Translational Link With Depression." *Biol Psychiatry* 90 (2): 118-127. https://doi.org/10.1016/j.biopsych.2021.04.004.

Bergmann, E., G. Zur, G. Bershadsky, and I. Kahn. 2016. "The Organization of Mouse and Human Cortico-Hippocampal Networks Estimated by Intrinsic Functional Connectivity." *Cereb Cortex* 26 (12): 4497-4512. https://doi.org/10.1093/cercor/bhw327.

Bleuler, Eugen. 1911. *Dementia praecox, oder Gruppe der Schizophrenien*. Vol. 1. Deuticke.

Bogerts, B., M. Ashtari, G. Degreef, J. M. Alvir, R. M. Bilder, and J. A. Lieberman. 1990. "Reduced temporal limbic structure volumes on magnetic resonance images in first episode schizophrenia." *Psychiatry Res* 35 (1): 1-13. https://doi.org/10.1016/0925-4927(90)90004-p.

Bygrave, A. M., K. Kilonzo, D. M. Kullmann, D. M. Bannerman, and D. Kätzel. 2019. "Can N-Methyl-D-Aspartate Receptor Hypofunction in Schizophrenia Be Localized to an Individual Cell Type?" *Front Psychiatry* 10: 835. https://doi.org/10.3389/fpsyt.2019.00835.

Carnemolla, S. E., J. W. Hsieh, R. Sipione, B. N. Landis, F. Kumfor, O. Piguet, and A. L. Manuel. 2020. "Olfactory dysfunction in frontotemporal dementia and psychiatric disorders: A systematic review." *Neurosci Biobehav Rev* 118: 588-611. https://doi.org/10.1016/j.neubiorev.2020.08.002.

Chen, Z. S., P. P. Kulkarni, I. R. Galatzer-Levy, B. Bigio, C. Nasca, and Y. Zhang. 2022. "Modern views of machine learning for precision psychiatry." *Patterns (N Y)* 3 (11): 100602. https://doi.org/10.1016/j.patter.2022.100602.

Chon, U., D. J. Vanselow, K. C. Cheng, and Y. Kim. 2019. "Enhanced and unified anatomical labeling for a common mouse brain atlas." *Nat Commun* 10 (1): 5067. https://doi.org/10.1038/s41467-019-13057-w.

Deng, K., L. Yang, J. Xie, H. Tang, G. S. Wu, and H. R. Luo. 2019. "Whole-brain mapping of projection from mouse lateral septal nucleus." *Biol Open* 8 (7). https://doi.org/10.1242/bio.043554.

Duarte, J. M. N., and L. Xin. 2019. "Magnetic Resonance Spectroscopy in Schizophrenia: Evidence for Glutamatergic Dysfunction and Impaired Energy Metabolism." *Neurochem Res* 44 (1): 102-116. https://doi.org/10.1007/s11064-018-2521-z.

Dwyer, D. B., P. Falkai, and N. Koutsouleris. 2018. "Machine Learning Approaches for Clinical Psychology and Psychiatry." *Annu Rev Clin Psychol* 14: 91-118. https://doi.org/10.1146/annurev-clinpsy-032816-045037.

Falkai, P., T. Schneider-Axmann, and W. G. Honer. 2000. "Entorhinal cortex pre-alpha cell clusters in schizophrenia: quantitative evidence of a developmental abnormality." *Biol Psychiatry* 47 (11): 937-43. https://doi.org/10.1016/s0006-3223(99)00250-4.

Fanselow, M. S., and H. W. Dong. 2010. "Are the dorsal and ventral hippocampus functionally distinct structures?" *Neuron* 65 (1): 7-19. https://doi.org/10.1016/j.neuron.2009.11.031.

Gaebel, Wolfgang. Wölwer, Wolfgang. 2010. "Schizophrenie." *Heft 50*.

Grace, A. A. 1991. "Phasic versus tonic dopamine release and the modulation of dopamine system responsivity: a hypothesis for the etiology of schizophrenia." *Neuroscience* 41 (1): 1-24. https://doi.org/10.1016/0306-4522(91)90196-u.

---. 2012. "Dopamine system dysregulation by the hippocampus: implications for the pathophysiology and treatment of schizophrenia." *Neuropharmacology* 62 (3): 1342-8. https://doi.org/10.1016/j.neuropharm.2011.05.011.

---. 2017. "Dopamine System Dysregulation and the Pathophysiology of Schizophrenia: Insights From the Methylazoxymethanol Acetate Model." *Biol Psychiatry* 81 (1): 5-8. https://doi.org/10.1016/j.biopsych.2015.11.007.

Harrison, P. J. 2004. "The hippocampus in schizophrenia: a review of the neuropathological evidence and its pathophysiological implications." *Psychopharmacology (Berl)* 174 (1): 151-62. https://doi.org/10.1007/s00213-003-1761-y.

Haukvik, U. K., L. T. Westlye, L. Mørch-Johnsen, K. N. Jørgensen, E. H. Lange, A. M. Dale, I. Melle, O. A. Andreassen, and I. Agartz. 2015. "In vivo hippocampal subfield volumes in schizophrenia and bipolar disorder." *Biol Psychiatry* 77 (6): 581-8. https://doi.org/10.1016/j.biopsych.2014.06.020.

Hecker, E. 1871. *Die Hebephrenie. Ein Beitrag zur klinischen Psychatrie* Berlin: Georg Reimer.

Heckers, S. 2001. "Neuroimaging studies of the hippocampus in schizophrenia." *Hippocampus* 11 (5): 520-8. https://doi.org/10.1002/hipo.1068.

Hjorthøj, C., A. E. Stürup, J. J. McGrath, and M. Nordentoft. 2017. "Years of potential life lost and life expectancy in schizophrenia: a systematic review and meta-analysis." *Lancet Psychiatry* 4 (4): 295-301. https://doi.org/10.1016/s2215-0366(17)30078-0.

Ho, N. F., J. E. Iglesias, M. Y. Sum, C. N. Kuswanto, Y. Y. Sitoh, J. De Souza, Z. Hong, B. Fischl, J. L. Roffman, J. Zhou, K. Sim, and D. J. Holt. 2017. "Progression from selective to general involvement of hippocampal subfields in schizophrenia." *Mol Psychiatry* 22 (1): 142-152. https://doi.org/10.1038/mp.2016.4.

Hobbiss, A. F., Y. Ramiro-Cortés, and I. Israely. 2018. "Homeostatic Plasticity Scales Dendritic Spine Volumes and Changes the Threshold and

Specificity of Hebbian Plasticity." *iScience* 8: 161-174. https://doi.org/10.1016/j.isci.2018.09.015.

Holthoff, K., Y. Kovalchuk, and A. Konnerth. 2006. "Dendritic spikes and activity-dependent synaptic plasticity." *Cell Tissue Res* 326 (2): 369-77. https://doi.org/10.1007/s00441-006-0263-8.

Huart, C., P. Rombaux, and T. Hummel. 2013. "Plasticity of the human olfactory system: the olfactory bulb." *Molecules* 18 (9): 11586-600. https://doi.org/10.3390/molecules180911586.

Huber, Gerd, Gisela Gross, and Reinhold Schüttler. 1979. "Verlaufs und sozialpsychiatrische Langzeituntersuchungen an den 1945–1959 in Bonn hospitalisierten schizophrenen Kranken." *Monogr Gesamtgeb Psychiatr Psychiatry Ser* 21: 1-399.

Janak, P. H., and K. M. Tye. 2015. "From circuits to behaviour in the amygdala." *Nature* 517 (7534): 284-92. https://doi.org/10.1038/nature14188.

Javitt, D. C., and S. R. Zukin. 1991. "Recent advances in the phencyclidine model of schizophrenia." *Am J Psychiatry* 148 (10): 1301-8. https://doi.org/10.1176/ajp.148.10.1301.

Jendryka, M., M. Palchaudhuri, D. Ursu, B. van der Veen, B. Liss, D. Katzel, W. Nissen, and A. Pekcec. 2019. "Pharmacokinetic and pharmacodynamic actions of clozapine-N-oxide, clozapine, and compound 21 in DREADD-based chemogenetics in mice." *Sci Rep* 9 (1): 4522. https://doi.org/10.1038/s41598-019-41088-2. https://www.ncbi.nlm.nih.gov/pubmed/30872749.

Kahlbaum, Karl Ludwig. 1874. *Die Katatonie oder das Spannungsirresein : eine klinische Form psychischer Krankheit*. Vol. 1*Klinische Abhandlungen über psychische Krankheiten*. Berlin: Hirschwald.

Kahn, I., J. R. Andrews-Hanna, J. L. Vincent, A. Z. Snyder, and R. L. Buckner. 2008. "Distinct cortical anatomy linked to subregions of the medial temporal lobe revealed by intrinsic functional connectivity." *J Neurophysiol* 100 (1): 129-39. https://doi.org/10.1152/jn.00077.2008.

Kahn, R. S., and I. E. Sommer. 2015. "The neurobiology and treatment of first-episode schizophrenia." *Mol Psychiatry* 20 (1): 84-97. https://doi.org/10.1038/mp.2014.66.

Kätzel, D., A. R. Wolff, A. M. Bygrave, and D. M. Bannerman. 2020. "Hippocampal Hyperactivity as a Druggable Circuit-Level Origin of Aberrant Salience in Schizophrenia." *Front Pharmacol* 11: 486811. https://doi.org/10.3389/fphar.2020.486811.

Keifer, O. P., Jr., R. C. Hurt, D. A. Gutman, S. D. Keilholz, S. L. Gourley, and K. J. Ressler. 2015. "Voxel-based morphometry predicts shifts in dendritic spine density and morphology with auditory fear conditioning." *Nat Commun* 6: 7582. https://doi.org/10.1038/ncomms8582.

Konradi, C., C. K. Yang, E. I. Zimmerman, K. M. Lohmann, P. Gresch, H. Pantazopoulos, S. Berretta, and S. Heckers. 2011. "Hippocampal interneurons are abnormal in schizophrenia." *Schizophr Res* 131 (1-3): 165-73. https://doi.org/10.1016/j.schres.2011.06.007.

Koutsouleris, N., E. M. Meisenzahl, S. Borgwardt, A. Riecher-Rössler, T. Frodl, J. Kambeitz, Y. Köhler, P. Falkai, H. J. Möller, M. Reiser, and C. Davatzikos. 2015. "Individualized differential diagnosis of schizophrenia and mood disorders using neuroanatomical biomarkers." *Brain* 138 (Pt 7): 2059-73. https://doi.org/10.1093/brain/awv111.

Kraepelin, E. 1909-1915. *Ein Lehrbuch für Studierende und Aertze. 8., vollständig umgearbeitete Auflage*. 8 vols. Vol. 8. Leipzig: Barth.

Kühn, S., F. Musso, A. Mobascher, T. Warbrick, G. Winterer, and J. Gallinat. 2012. "Hippocampal subfields predict positive symptoms in schizophrenia: first evidence from brain morphometry." *Transl Psychiatry* 2 (6): e127. https://doi.org/10.1038/tp.2012.51.

Lieberman, J. A., R. R. Girgis, G. Brucato, H. Moore, F. Provenzano, L. Kegeles, D. Javitt, J. Kantrowitz, M. M. Wall, C. M. Corcoran, S. A. Schobel, and S. A. Small. 2018. Hippocampal dysfunction in the pathophysiology of schizophrenia: a selective review and hypothesis for early detection and intervention. In *Mol Psychiatry*.

Lisman, J. E., J. T. Coyle, R. W. Green, D. C. Javitt, F. M. Benes, S. Heckers, and A. A. Grace. 2008. "Circuit-based framework for understanding neurotransmitter and risk gene interactions in schizophrenia." *Trends Neurosci* 31 (5): 234-42. https://doi.org/10.1016/j.tins.2008.02.005.

Lisman, J. E., and A. A. Grace. 2005. "The hippocampal-VTA loop: controlling the entry of information into long-term memory." *Neuron* 46 (5): 703-13. https://doi.org/10.1016/j.neuron.2005.05.002.

Lodge, D. J., and A. A. Grace. 2007. "Aberrant hippocampal activity underlies the dopamine dysregulation in an animal model of schizophrenia." *J Neurosci* 27 (42): 11424-30. https://doi.org/10.1523/jneurosci.2847-07.2007.

Lu, Chenyue, Di Jin, Nathan Palmer, Kathe Fox, Isaac S. Kohane, Jordan W. Smoller, and Kun-Hsing Yu. 2022. "Large-scale real-world data analysis identifies comorbidity patterns in schizophrenia." *Translational Psychiatry* 12 (1): 154. https://doi.org/10.1038/s41398-022-01916-y. https://doi.org/10.1038/s41398-022-01916-y.

Mailman, R. B., and V. Murthy. 2010. "Third generation antipsychotic drugs: partial agonism or receptor functional selectivity?" *Curr Pharm Des* 16 (5): 488-501. https://doi.org/10.2174/138161210790361461.

Mathew, I., T. M. Gardin, N. Tandon, S. Eack, A. N. Francis, L. J. Seidman, B. Clementz, G. D. Pearlson, J. A. Sweeney, C. A. Tamminga, and M. S. Keshavan. 2014. "Medial temporal lobe structures and hippocampal subfields in psychotic disorders: findings from the Bipolar-Schizophrenia Network on Intermediate Phenotypes (B-SNIP) study." *JAMA Psychiatry* 71 (7): 769-77. https://doi.org/10.1001/jamapsychiatry.2014.453.

McDonald, A. J., and D. D. Mott. 2017. "Functional neuroanatomy of amygdalohippocampal interconnections and their role in learning and memory." *J Neurosci Res* 95 (3): 797-820. https://doi.org/10.1002/jnr.23709.

McHugo, M., P. Talati, N. D. Woodward, K. Armstrong, J. U. Blackford, and S. Heckers. 2018. "Regionally specific volume deficits along the hippocampal long axis in early and chronic psychosis." *Neuroimage Clin* 20: 1106-1114. https://doi.org/10.1016/j.nicl.2018.10.021.

Miranda, M., J. F. Morici, M. B. Zanoni, and P. Bekinschtein. 2019. "Brain-Derived Neurotrophic Factor: A Key Molecule for Memory in the Healthy and the Pathological Brain." *Front Cell Neurosci* 13: 363. https://doi.org/10.3389/fncel.2019.00363.

Moberg, P. J., R. Agrin, R. E. Gur, R. C. Gur, B. I. Turetsky, and R. L. Doty. 1999. "Olfactory dysfunction in schizophrenia: a qualitative and quantitative review." *Neuropsychopharmacology* 21 (3): 325-40. https://doi.org/10.1016/s0893-133x(99)00019-6.

Moberg, P. J., V. Kamath, D. M. Marchetto, M. E. Calkins, R. L. Doty, C. G. Hahn, K. E. Borgmann-Winter, C. G. Kohler, R. E. Gur, and B. I. Turetsky. 2014. "Meta-analysis of olfactory function in schizophrenia, first-degree family members, and youths at-risk for psychosis." *Schizophr Bull* 40 (1): 50-9. https://doi.org/10.1093/schbul/sbt049.

Nakahara, S., M. Matsumoto, and T. G. M. van Erp. 2018. "Hippocampal subregion abnormalities in schizophrenia: A systematic review of structural and physiological imaging studies." *Neuropsychopharmacol Rep* 38 (4): 156-166. https://doi.org/10.1002/npr2.12031. https://www.ncbi.nlm.nih.gov/pubmed/30255629.

National Institute of Mental Health, NIMH 2022. "Research Domain Criteria Initiative (RDoC) ". U.S. Department of Health and Human Services, National Institute of Mental Health https://www.nimh.nih.gov/research/research-funded-by-nimh/rdoc/about-rdoc.

Nelson, M. D., A. J. Saykin, L. A. Flashman, and H. J. Riordan. 1998. "Hippocampal volume reduction in schizophrenia as assessed by magnetic resonance imaging: a meta-analytic study." *Arch Gen Psychiatry* 55 (5): 433-40. https://doi.org/10.1001/archpsyc.55.5.433.

Neves, G., S. F. Cooke, and T. V. Bliss. 2008. "Synaptic plasticity, memory and the hippocampus: a neural network approach to causality." *Nat Rev Neurosci* 9 (1): 65-75. https://doi.org/10.1038/nrn2303.

Newcomer, J. W., N. B. Farber, and J. W. Olney. 2000. "NMDA receptor function, memory, and brain aging." *Dialogues Clin Neurosci* 2 (3): 219-32. https://doi.org/10.31887/DCNS.2000.2.3/jnewcomer.

Nguyen, R., M. D. Morrissey, V. Mahadevan, J. D. Cajanding, M. A. Woodin, J. S. Yeomans, K. Takehara-Nishiuchi, and J. C. Kim. 2014. "Parvalbumin and GAD65 interneuron inhibition in the ventral hippocampus induces distinct behavioral deficits relevant to schizophrenia." *J Neurosci* 34 (45): 14948-60. https://doi.org/10.1523/jneurosci.2204-14.2014.

NIH. 2020. "Schizophrenia." https://www.nimh.nih.gov/health/topics/schizophrenia/.

Olbrich, H. G., and H. Braak. 1985. "Ratio of pyramidal cells versus non-pyramidal cells in sector CA1 of the human Ammon's horn." *Anat Embryol (Berl)* 173 (1): 105-10. https://doi.org/10.1007/bf00707308.

Padmanabhan, K., F. Osakada, A. Tarabrina, E. Kizer, E. M. Callaway, F. H. Gage, and T. J. Sejnowski. 2018. "Centrifugal Inputs to the Main Olfactory Bulb Revealed Through Whole Brain Circuit-Mapping." *Front Neuroanat* 12: 115. https://doi.org/10.3389/fnana.2018.00115.

Pantelis, C., D. Velakoulis, P. D. McGorry, S. J. Wood, J. Suckling, L. J. Phillips, A. R. Yung, E. T. Bullmore, W. Brewer, B. Soulsby, P. Desmond, and P. K. McGuire. 2003. "Neuroanatomical abnormalities before and after onset of psychosis: a cross-sectional and longitudinal MRI comparison." *Lancet* 361 (9354): 281-8. https://doi.org/10.1016/s0140-6736(03)12323-9.

Radley, J. J., H. M. Sisti, J. Hao, A. B. Rocher, T. McCall, P. R. Hof, B. S. McEwen, and J. H. Morrison. 2004. "Chronic behavioral stress induces apical dendritic reorganization in pyramidal neurons of the medial prefrontal cortex." *Neuroscience* 125 (1): 1-6. https://doi.org/10.1016/j.neuroscience.2004.01.006.

Redlich, R., J. J. Almeida, D. Grotegerd, N. Opel, H. Kugel, W. Heindel, V. Arolt, M. L. Phillips, and U. Dannlowski. 2014. "Brain morphometric biomarkers distinguishing unipolar and bipolar depression. A voxel-based morphometry-pattern classification approach." *JAMA Psychiatry* 71 (11): 1222-30. https://doi.org/10.1001/jamapsychiatry.2014.1100.

Ripke, Stephan, Benjamin M. Neale, Aiden Corvin, James T. R. Walters, Kai-How Farh, Peter A. Holmans, Phil Lee, Brendan Bulik-Sullivan, David A. Collier, Hailiang Huang, Tune H. Pers, Ingrid Agartz, Esben Agerbo, Margot Albus, Madeline Alexander, Farooq Amin, Silviu A. Bacanu, Martin Begemann, Richard A. Belliveau Jr, Judit Bene, Sarah E. Bergen, Elizabeth Bevilacqua, Tim B. Bigdeli, Donald W. Black, Richard Bruggeman, Nancy G. Buccola, Randy L. Buckner, William Byerley, Wiepke Cahn, Guiqing Cai, Dominique Campion, Rita M. Cantor, Vaughan J. Carr, Noa Carrera, Stanley V. Catts, Kimberly D. Chambert, Raymond C. K. Chan, Ronald Y. L. Chen, Eric Y. H. Chen, Wei Cheng, Eric F. C. Cheung, Siow Ann Chong, C. Robert Cloninger, David Cohen, Nadine Cohen, Paul Cormican, Nick Craddock, James J. Crowley, David Curtis, Michael Davidson, Kenneth L. Davis, Franziska Degenhardt, Jurgen Del Favero, Ditte Demontis, Dimitris Dikeos, Timothy Dinan, Srdjan Djurovic, Gary Donohoe, Elodie Drapeau, Jubao Duan, Frank Dudbridge, Naser Durmishi, Peter Eichhammer, Johan Eriksson, Valentina Escott-Price, Laurent Essioux, Ayman H. Fanous, Martilias S. Farrell, Josef Frank, Lude Franke, Robert Freedman, Nelson B. Freimer, Marion Friedl, Joseph I. Friedman, Menachem Fromer, Giulio Genovese, Lyudmila Georgieva, Ina Giegling, Paola Giusti-Rodríguez, Stephanie Godard, Jacqueline I. Goldstein, Vera Golimbet, Srihari Gopal, Jacob Gratten, Lieuwe de Haan, Christian Hammer, Marian L. Hamshere, Mark Hansen, Thomas Hansen, Vahram Haroutunian, Annette M. Hartmann, Frans A. Henskens, Stefan Herms, Joel N. Hirschhorn, Per Hoffmann, Andrea Hofman, Mads V. Hollegaard, David M. Hougaard, Masashi Ikeda, Inge Joa, Antonio Julià, René S. Kahn, Luba Kalaydjieva, Sena Karachanak-Yankova, Juha Karjalainen, David Kavanagh, Matthew C. Keller, James L. Kennedy, Andrey Khrunin, Yunjung Kim, Janis Klovins, James A. Knowles, Bettina Konte, Vaidutis Kucinskas, Zita Ausrele Kucinskiene, Hana Kuzelova-Ptackova, Anna K. Kähler, Claudine Laurent, Jimmy Lee Chee Keong, S. Hong Lee, Sophie E. Legge, Bernard Lerer, Miaoxin Li, Tao Li, Kung-Yee Liang, Jeffrey Lieberman, Svetlana Limborska, Carmel M. Loughland, Jan Lubinski, Jouko Lönnqvist, Milan Macek Jr, Patrik K. E. Magnusson, Brion S. Maher, Wolfgang Maier, Jacques Mallet, Sara Marsal, Manuel Mattheisen, Morten Mattingsdal, Robert W. McCarley, Colm McDonald, Andrew M. McIntosh, Sandra Meier, Carin J. Meijer, Bela Melegh, Ingrid Melle, Raquelle I. Mesholam-Gately, Andres Metspalu, Patricia T. Michie, Lili Milani, Vihra Milanova, Younes Mokrab, Derek W. Morris, Ole Mors, Kieran C. Murphy, Robin M. Murray, Inez Myin-Germeys, Bertram Müller-Myhsok, Mari Nelis, Igor Nenadic, Deborah A. Nertney, Gerald Nestadt, Kristin K. Nicodemus, Liene Nikitina-Zake, Laura Nisenbaum, Annelie Nordin, Eadbhard O'Callaghan, Colm O'Dushlaine, F. Anthony O'Neill, Sang-Yun Oh, Ann Olincy, Line Olsen, Jim Van Os, Christos Pantelis, George N. Papadimitriou, Sergi Papiol, Elena Parkhomenko, Michele T. Pato, Tiina Paunio, Milica Pejovic-Milovancevic, Diana O. Perkins, Olli Pietiläinen, Jonathan Pimm, Andrew J. Pocklington, John Powell, Alkes Price, Ann E. Pulver, Shaun M. Purcell, Digby Quested, Henrik B. Rasmussen, Abraham Reichenberg, Mark A. Reimers, Alexander L. Richards, Joshua L. Roffman, Panos Roussos, Douglas M. Ruderfer, Veikko Salomaa, Alan R. Sanders, Ulrich Schall, Christian R. Schubert,

Thomas G. Schulze, Sibylle G. Schwab, Edward M. Scolnick, Rodney J. Scott, Larry J. Seidman, Jianxin Shi, Engilbert Sigurdsson, Teimuraz Silagadze, Jeremy M. Silverman, Kang Sim, Petr Slominsky, Jordan W. Smoller, Hon-Cheong So, ChrisC A. Spencer, Eli A. Stahl, Hreinn Stefansson, Stacy Steinberg, Elisabeth Stogmann, Richard E. Straub, Eric Strengman, Jana Strohmaier, T. Scott Stroup, Mythily Subramaniam, Jaana Suvisaari, Dragan M. Svrakic, Jin P. Szatkiewicz, Erik Söderman, Srinivas Thirumalai, Draga Toncheva, Sarah Tosato, Juha Veijola, John Waddington, Dermot Walsh, Dai Wang, Qiang Wang, Bradley T. Webb, Mark Weiser, Dieter B. Wildenauer, Nigel M. Williams, Stephanie Williams, Stephanie H. Witt, Aaron R. Wolen, Emily H. M. Wong, Brandon K. Wormley, Hualin Simon Xi, Clement C. Zai, Xuebin Zheng, Fritz Zimprich, Naomi R. Wray, Kari Stefansson, Peter M. Visscher, Wellcome Trust Case-Control Consortium, Rolf Adolfsson, Ole A. Andreassen, Douglas H. R. Blackwood, Elvira Bramon, Joseph D. Buxbaum, Anders D. Børglum, Sven Cichon, Ariel Darvasi, Enrico Domenici, Hannelore Ehrenreich, Tõnu Esko, Pablo V. Gejman, Michael Gill, Hugh Gurling, Christina M. Hultman, Nakao Iwata, Assen V. Jablensky, Erik G. Jönsson, Kenneth S. Kendler, George Kirov, Jo Knight, Todd Lencz, Douglas F. Levinson, Qingqin S. Li, Jianjun Liu, Anil K. Malhotra, Steven A. McCarroll, Andrew McQuillin, Jennifer L. Moran, Preben B. Mortensen, Bryan J. Mowry, Markus M. Nöthen, Roel A. Ophoff, Michael J. Owen, Aarno Palotie, Carlos N. Pato, Tracey L. Petryshen, Danielle Posthuma, Marcella Rietschel, Brien P. Riley, Dan Rujescu, Pak C. Sham, Pamela Sklar, David St Clair, Daniel R. Weinberger, Jens R. Wendland, Thomas Werge, Consortium Schizophrenia Working Group of the Psychiatric Genomics, and Consortium Psychosis Endophenotypes International. 2014. "Biological insights from 108 schizophrenia-associated genetic loci." *Nature* 511 (7510): 421-427. https://doi.org/10.1038/nature13595. https://doi.org/10.1038/nature13595.

Schneider, Kurt. 1950. *Klinische Psychopathologie*. Stuttgart: Thieme.

Schobel, S. A., N. H. Chaudhury, U. A. Khan, B. Paniagua, M. A. Styner, I. Asllani, B. P. Inbar, C. M. Corcoran, J. A. Lieberman, H. Moore, and S. A. Small. 2013. "Imaging patients with psychosis and a mouse model establishes a spreading pattern of hippocampal dysfunction and implicates glutamate as a driver." *Neuron* 78 (1): 81-93. https://doi.org/10.1016/j.neuron.2013.02.011. https://www.ncbi.nlm.nih.gov/pubmed/23583108.

Sierra, A., S. Martín-Suárez, R. Valcárcel-Martín, J. Pascual-Brazo, S. A. Aelvoet, O. Abiega, J. J. Deudero, A. L. Brewster, I. Bernales, A. E. Anderson, V. Baekelandt, M. Maletić-Savatić, and J. M. Encinas. 2015. "Neuronal hyperactivity accelerates depletion of neural stem cells and impairs hippocampal neurogenesis." *Cell Stem Cell* 16 (5): 488-503. https://doi.org/10.1016/j.stem.2015.04.003.

Simmons, J. M., and K. J. Quinn. 2014. "The NIMH Research Domain Criteria (RDoC) Project: implications for genetics research." *Mamm Genome* 25 (1-2): 23-31. https://doi.org/10.1007/s00335-013-9476-9.

Small, S. A., S. A. Schobel, R. B. Buxton, M. P. Witter, and C. A. Barnes. 2011. "A pathophysiological framework of hippocampal dysfunction in ageing and disease." *Nat Rev Neurosci* 12 (10): 585-601. https://doi.org/10.1038/nrn3085.

Sørensen, H. J., E. L. Mortensen, J. Schiffman, J. M. Reinisch, J. Maeda, and S. A. Mednick. 2010. "Early developmental milestones and risk of schizophrenia: a 45-year follow-up of the Copenhagen Perinatal Cohort." *Schizophr Res* 118 (1-3): 41-7. https://doi.org/10.1016/j.schres.2010.01.029.

Stampanoni Bassi, M., E. Iezzi, L. Gilio, D. Centonze, and F. Buttari. 2019. "Synaptic Plasticity Shapes Brain Connectivity: Implications for Network Topology." *Int J Mol Sci* 20 (24). https://doi.org/10.3390/ijms20246193.

Stepniak, B., S. Papiol, C. Hammer, A. Ramin, S. Everts, L. Hennig, M. Begemann, and H. Ehrenreich. 2014. "Accumulated environmental risk determining age at schizophrenia onset: a deep phenotyping-based study." *Lancet Psychiatry* 1 (6): 444-53. https://doi.org/10.1016/s2215-0366(14)70379-7.

Stępnicki, P., M. Kondej, and A. A. Kaczor. 2018. "Current Concepts and Treatments of Schizophrenia." *Molecules* 23 (8). https://doi.org/10.3390/molecules23082087.

Stilo, S. A., and R. M. Murray. 2019. "Non-Genetic Factors in Schizophrenia." *Curr Psychiatry Rep* 21 (10): 100. https://doi.org/10.1007/s11920-019-1091-3.

van Groen, T., P. Miettinen, and I. Kadish. 2003. "The entorhinal cortex of the mouse: organization of the projection to the hippocampal formation." *Hippocampus* 13 (1): 133-49. https://doi.org/10.1002/hipo.10037.

Wellman, C. L. 2001. "Dendritic reorganization in pyramidal neurons in medial prefrontal cortex after chronic corticosterone administration." *J Neurobiol* 49 (3): 245-53. https://doi.org/10.1002/neu.1079.

Willner, P. 1986. "Validation criteria for animal models of human mental disorders: learned helplessness as a paradigm case." *Prog Neuropsychopharmacol Biol Psychiatry* 10 (6): 677-90. https://doi.org/10.1016/0278-5846(86)90051-5.

Zhou, G., J. K. Olofsson, M. Z. Koubeissi, G. Menelaou, J. Rosenow, S. U. Schuele, P. Xu, J. L. Voss, G. Lane, and C. Zelano. 2021. "Human

hippocampal connectivity is stronger in olfaction than other sensory systems." *Prog Neurobiol* 201: 102027. https://doi.org/10.1016/j.pneurobio.2021.102027.

Zubin, Joseph, and Bonnie Spring. 1977. "Vulnerability: a new view of schizophrenia." *Journal of abnormal psychology* 86 (2): 103.

Additionally, software, including ChatGPT developed by OpenAI in San Francisco, USA (2025), was used exclusively for assistance in sentence editing. No content generation, data analysis, or scientific input was provided.

Acknowledgment

Many people have helped me in the realisation of this dissertation, to whom I would like to express my sincerest gratitude.

First, I would like to thank PD Dr. Carsten Wotjak, who took me on as an MD student in the final phase of his research group at the Max Plank Institute. He supported me greatly with his enormous expertise and knowledge in the realisation of this project. As members of the doctoral committee, I would also like to thank Prof. Dr. Nikolaos Koutsouleris for his helpful and inspirational input and encouragement in terms of neuroimaging and Prof. Dr. Moritz Rossner for his support and contribution.

I would like to say a special thank you to my direct supervisor Daniel E. Heinz, who has, in close cooperation, contributed greatly to the project with his daily efforts. Besides numerous practical skills in the laboratory, I have learned a lot of administrative and communication skills that have been essential for the realisation of the project and the collaboration between the different core units. Thank you very much for your exceptional commitment and constant availability!

For the cooperation and support in terms of neuroimaging I would like to thank Dr. Michael Czisch and Tibor Stark. They taught me a lot about the technical background of the MRI, its evaluation and execution.

For instructing and helping me with the stereotactic operations, I would also like to thank Dr. Rosa Eva Hüttle and Julia Ruat for her help with the IHC.

Finally, I would like to express my deepest gratitude to my family and partner, who have accompanied and supported me throughout this time. This has been an enormous asset and source of energy, which I will always appreciate.

LMU LUDWIG-MAXIMILIANS-UNIVERSITÄT MÜNCHEN

Dekanat Medizinische Fakultät
Promotionsbüro

Erklärung zur Übereinstimmung der gebundenen Ausgabe der Dissertation mit der elektronischen Fassung

Bartmann, Lea Marleen Joanna

Name, Vorname

Hiermit erkläre ich, dass die elektronische Version der eingereichten Dissertation mit dem Titel:

Do Long-Term Changes in Neuronal Activity translate into Changes in Grey Matter Volume?

in Inhalt und Formatierung mit den gedruckten und gebundenen Exemplaren übereinstimmt.

Berlin, 18.11.2025
Ort, Datum

Lea Bartmann
Unterschrift Lea Marleen Joanna Bartmann

Eidesstattliche Versicherung

Bartmann, Lea Marleen Joanna

Name, Vorname

Ich erkläre hiermit an Eides statt, dass ich die vorliegende Dissertation mit dem Titel

Do Long-Term Changes in Neuronal Activity translate into Changes in Grey Matter Volume?

selbständig verfasst, mich außer der angegebenen keiner weiteren Hilfsmittel bedient und alle Erkenntnisse, die aus dem Schrifttum ganz oder annähernd übernommen sind, als solche kenntlich gemacht und nach ihrer Herkunft unter Bezeichnung der Fundstelle einzeln nachgewiesen habe.

Ich erkläre des Weiteren, dass die hier vorgelegte Dissertation nicht in gleicher oder in ähnlicher Form bei einer anderen Stelle zur Erlangung eines akademischen Grades eingereicht wurde.

Berlin, 18.11.2025
Ort, Datum

Lea Bartmann
Unterschrift Lea Marleen Joanna Bartmann